

# Chapter 5

## Phenomenological Theory I: Nuclear $\beta$ -decays and Weak Interaction of Leptons

### 5.1 Introduction

The history of the phenomenological theory of neutrino interactions and weak interactions in general, begins with the attempts to understand the physics of nuclear radiation known as  $\beta$ -rays. These highly penetrating and ionizing component of the radiation discovered by Becquerel [9] in 1896 were subsequently established to be electrons by doing many experiments in which their properties like charge, mass, and energy were studied [8]. Since the energy of these  $\beta$ -ray electrons was found to be in the range of a few MeV, they were believed to be of nuclear origin in the light of the basic structure of the nucleus known at that time [4]. It was assumed that the electrons are emitted in a nuclear process called  $\beta$ -decay in which a nucleus in the initial state goes to a final state by emitting an electron. The energy distribution of the  $\beta$ -ray electrons was found to be continuous lying between  $m_e$ , the mass of the electron, and a maximum energy  $E_{\max}$  corresponding to the available energy in the nuclear  $\beta$ -decay, that is,  $E_{\max} = E_i - E_f$ , where  $E_i$  and  $E_f$  are the energies of the initial and final nuclear states. A typical continuous energy distribution for the electrons from the  $\beta$ -decay of RaE is shown in Figure 1.1 of Chapter 1. It was first thought that the electrons in the  $\beta$ -decay process were emitted with a fixed energy  $E_{\max}$  and suffered random losses in their energy due to secondary interactions with nuclear constituents as they traveled through the nucleus before being observed leading to a continuous energy distribution. However, the calorimetric heat measurements performed by Ellis et al. [15] and confirmed later by Meitner et al. [16] in the  $\beta$ -decays of RaE, established that the electrons emitted in the process of the nuclear  $\beta$ -decay have an intrinsically continuous energy distribution. The continuous energy distribution of the electrons from the  $\beta$ -decay posed a difficult problem toward its theoretical interpretation in the context of the contemporary model of the nuclear structure and seemed to violate the law of conservation of energy. In order to save the law of energy conservation, Pauli proposed in

1930 [1], the existence of a new, neutral, almost massless, spin  $\frac{1}{2}$  particle which was assumed to be emitted along with the electron in the  $\beta$ -decay and share the available energy with the electron leading to the continuous energy distribution of the electron. The new particle was later named neutrino by Fermi [219] and a theory of the nuclear  $\beta$ -decay was given for the first time by Fermi [219] and independently by Perrin [24] in 1933. The theory was extended by Gamow and Teller [26] and Bethe and Bacher [27] in order to understand other types of nuclear  $\beta$ -decays, which were observed later. It was followed by a large amount of experimental and theoretical works on  $\beta$ -decays and other weak interaction processes of elementary particles and nuclei before a phenomenological theory of weak interactions was formulated. The experimental determination of the various parameters of the phenomenological theory took almost 20 years leading to the  $V - A$  theory of weak interactions [41, 42, 43]. During this period, many landmark discoveries in physics like parity violation in weak interactions, two-component neutrinos, neutrino helicities, lepton number and its conservation, and the existence of more than one neutrino flavor were made. The  $V - A$  theory was later extended to the strangeness sector by Cabibbo [59] in 1963, to the charm sector by Glashow–Iliopoulos–Maiani (GIM) [64] in 1970, and to the heavy quark flavor sector by Kobayashi and Maskawa [70] in 1973. The phenomenological theory was quite successful in explaining the weak interaction processes at low energies but faced many difficulties when extended to higher energies due to the divergences in higher orders and non-renormalizability of the theory. However, the  $V - A$  theory implied the existence of massive vector bosons as mediators of weak interactions; these bosons played an important role in the formulation of the standard model of the unified theory of the electromagnetic and weak interactions [220, 157, 37].

In the following sections, we describe the experimental and theoretical developments in the study of nuclear  $\beta$ -decays and weak decays of leptons leading to the  $V - A$  theory of weak interactions and its application to weak processes [221, 222]. We also include a separate section at the end of this chapter which describes the limitations of the  $V - A$  theory.

## 5.2 Development of Phenomenological Theory

### 5.2.1 Fermi and Gamow–Teller theories of $\beta$ -decays

Fermi [219] proposed the theory of the nuclear  $\beta$ -decay in analogy with quantum electrodynamics (QED), the theory of electromagnetic interactions in which a photon is created in the interaction between a charged particle and the electromagnetic field according to the principles of creation and annihilation of particles in quantum field theory (QFT) as shown in Figure 5.1.

The interaction Hamiltonian density  $\mathcal{H}_{\text{int}}^{\text{em}}(x)$  for the electromagnetic interaction of a charged particle, say electron (with charge  $e$ ) with the electromagnetic field  $A^\mu(x)$  is written in QED as a scalar product of the four-component electromagnetic current  $j_\mu^{\text{em}}(x)$  and the four-component electromagnetic field  $A^\mu(x)$ , that is,

$$\mathcal{H}_{\text{int}}^{\text{em}}(x) = ej_\mu(x)A^\mu(x), \quad (5.1)$$

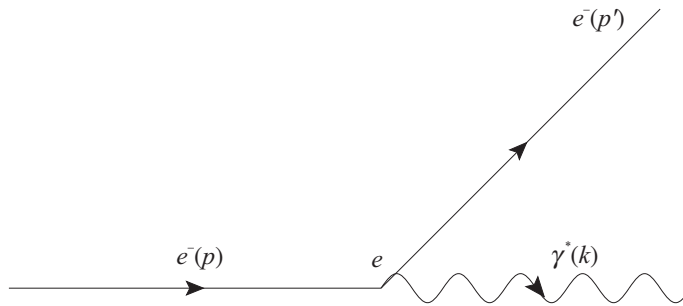


**Figure 5.1** Interaction of a charged particle with the electromagnetic field.

where

$$j_\mu(x) = \bar{\psi}_e(x) \gamma_\mu \psi_e(x), \quad (5.2)$$

and  $e = \sqrt{4\pi\alpha}$ , with  $\alpha (= \frac{1}{137})$  being the fine structure constant. The function  $\psi_e(x)$  is the spin  $\frac{1}{2}$  field of the electron which satisfies the Dirac equation, that is,

$$\left( i\gamma^\mu \frac{\partial}{\partial x^\mu} - m \right) \psi_e(x) = 0 \quad (5.3)$$

and is expressed in terms of the Dirac spinor, and the four momenta of the particle  $(E, \vec{p})$ , as:

$$\psi_e(x) = N u_e(\vec{p}) e^{-i(Et - \vec{p} \cdot \vec{x})}, \quad (5.4)$$

where  $N$  is the normalization factor and  $u_e$  is a four-component Dirac spinor given by:

$$u_e = \begin{pmatrix} 1 \\ \frac{\vec{\sigma} \cdot \vec{p}}{E + M} \end{pmatrix} \chi_e^s. \quad (5.5)$$

Here,  $\vec{\sigma}$  is the Pauli spin operator and  $\chi_e^s$  is a two-component spin wave function of the electron corresponding to the spin up ( $S = \frac{1}{2}, S_z = +\frac{1}{2}$ ) and spin down ( $S = \frac{1}{2}, S_z = -\frac{1}{2}$ ) states of the electron.

The interaction described by the Hamiltonian density given in Eq. (5.1) is diagrammatically represented by the Feynman diagram shown in Figure 5.1, where the direction of the arrow shows the direction of the electromagnetic current  $j_\mu(x)$  of the electron with initial momentum  $p^\mu$  and final momentum  $p'^\mu$  interacting with the electromagnetic field  $A^\mu(x)$  at space-time  $x$  creating a photon of momentum  $k^\mu$  such that  $p^\mu = p'^\mu + k^\mu$ , with strength  $e$ .

In analogy with QED, Fermi assumed that, in the process of  $\beta$ -decay, a neutron in the nucleus is converted into a proton by creating a pair of electron and neutrino (established later as an antineutrino) from the physical vacuum through a weak interaction process:

$$n(p) \rightarrow p(p') + e^-(k') + \bar{\nu}_e(k), \quad (5.6)$$

where the quantities in the bracket are the four momenta of the respective particles. He wrote the  $\beta$ -decay Hamiltonian density as [223]:

$$\begin{aligned}\mathcal{H}_{\text{int}}^{\text{Fermi}}(x) &= G\bar{\psi}_e\gamma_\mu(x)\psi_\nu(x) \times \bar{\psi}_p(x)\gamma^\mu\psi_n(x) + h.c. \\ &= G j_\mu^e(x) j_h^\mu(x),\end{aligned}\quad (5.7)$$

which assumes that the interaction is a scalar product of the two vector currents, that is, a lepton 4-component vector current,  $j_\mu^e(x) = \bar{\psi}_e(x)\gamma_\mu\psi_\nu(x)$  and a 4-component vector nucleon current  $j_h^\mu(x) = \bar{\psi}_p(x)\gamma^\mu\psi_n(x)$ . For this reason, it is called a current–current interaction of  $\beta$ -decay. It is also called a four Fermi point interaction because there are four spin  $\frac{1}{2}$  fermion fields of proton, neutron, electron, and antineutrino described by the function  $\psi_i(x)$  ( $i = n, p, e, \bar{\nu}_e$ ) given in Eq. (5.4) interacting at the space–time point  $x$ . The strength of the interaction is described by the coupling constant  $G$  which has the dimension of  $(\text{mass})^{-2}$  in contrast to the electromagnetic interaction, where strength of the coupling  $e(= \sqrt{4\pi\alpha})$  is dimensionless. Diagrammatically, the interaction described by Eq. (5.7), is represented by the Feynman diagram shown in Figure 5.2. Here a nucleon current  $j_h^\mu(x)$ , in which a neutron of momentum  $p^\mu$  is converted into a proton of momentum  $p'^\mu$ , interacts with a lepton current  $j_\mu^e(x)$  with strength  $G$ , in which an electron of momentum  $k'^\nu$  and antineutrino of momentum  $k^\nu$  is created (or equivalently, a neutrino of momentum  $k^\nu$  is annihilated) such that:

$$p^\nu = p'^\nu + k^\nu + k'^\nu = p'^\nu + q^\nu \quad \text{with} \quad q^\nu = k^\nu + k'^\nu, \quad (5.8)$$

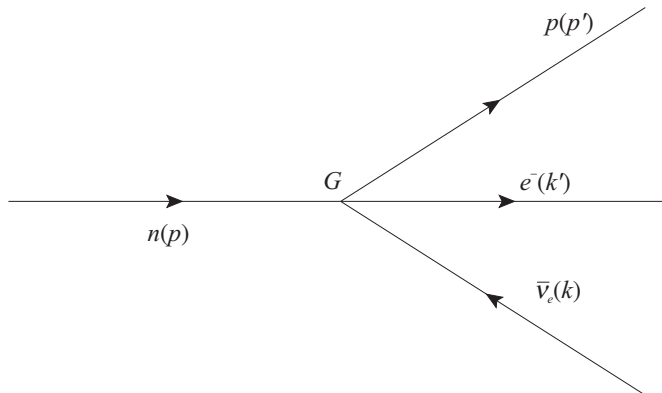


**Figure 5.2** Four point Fermi interaction.

at the space–time point  $x$ . It should be noted that in the weak interaction process of  $\beta$ -decay, both currents, that is, the nucleon and the lepton currents carry charge of one unit unlike the electromagnetic current, that is,  $j_\mu^{\text{em}}(x)$  which carries no charge. The weak currents in the  $\beta$ -decay are, therefore, known as charge changing (CC) weak currents.

In the case of nuclear  $\beta$ -decays, a neutron inside a nucleus at the initial state  $|i\rangle$  decays into a proton defined by a final state  $|f\rangle$ , and a pair of electron and antineutrino is created in the

interaction. The  $S$  matrix for the process, in the Fermi theory, is given by:

$$\begin{aligned} S &= -i \langle f | \int dt H_{\text{int}}^{\text{Fermi}}(t) | i \rangle = i \langle f | \int d^4x \mathcal{L}_{\text{int}}^{\text{Fermi}}(x) | i \rangle \\ &= iG \langle f | \int d^4x \left\{ \bar{\psi}_e(x) \gamma_\mu \psi_\nu(x) \bar{\psi}_p(x) \gamma^\mu \psi_n(x) + h.c. \right\} | i \rangle, \end{aligned} \quad (5.9)$$

where  $\psi_n(x)$ ,  $\psi_p(x)$ ,  $\psi_e(x)$ , and  $\psi_\nu(x)$  are the wave functions of neutrons, protons, electrons, and neutrinos given by:

$$\psi_n(x) = \frac{1}{\sqrt{2E_n V}} \psi_n(\vec{x}) e^{-iE_n t}, \quad (5.10)$$

$$\psi_p(x) = \frac{1}{\sqrt{2E_p V}} \psi_p(\vec{x}) e^{-iE_p t}, \quad (5.11)$$

$$\psi_e(x) = \frac{1}{\sqrt{2E_e V}} \psi_e(\vec{x}) e^{-iE_e t}, \quad (5.12)$$

$$\psi_\nu(x) = \frac{1}{\sqrt{2E_\nu V}} \psi_\nu(\vec{x}) e^{-iE_\nu t}. \quad (5.13)$$

In nuclear  $\beta$ -decay, the neutrons and protons are bound in the nucleus and the electron moves in the Coulomb field of the final nucleus after being created in the process of  $\beta$ -decay. The electron–neutrino pair created in the process carries an energy in the region of a few MeV resulting in a very small, almost negligible recoil energy of the nucleus  $\left( \simeq \frac{(|\vec{k} + \vec{k}'|)^2}{2AM} \simeq \text{a few keV} \right)$ . Therefore, the final nucleus along with the initial nucleus can be considered to be at rest. Moreover, the nucleons bound in the nucleus move with their Fermi momentum corresponding to a kinetic energy of about 8–10 MeV and can be treated non-relativistically. This allows us to take the non-relativistic limit of the hadronic current  $j_h^\mu(x)$  using the following form of the wave functions  $\psi_n(x)$  and  $\psi_p(x)$ , for the neutron and proton respectively, apart from a normalization factor, that is,

$$\psi_{p,n}(\vec{x}) = \left( \frac{1}{\frac{\vec{\sigma} \cdot \vec{p}}{E+M}} \right) \phi_{p,n}(\vec{x}). \quad (5.14)$$

In the limit  $\vec{p} \rightarrow 0$  (Appendix A),

$$\begin{aligned} \bar{\psi}_p(\vec{x}) \gamma^\mu \psi_n(\vec{x}) &\rightarrow \phi_p^\dagger(\vec{x}) \mathbb{1} \phi_n(\vec{x}), \quad \text{when } \mu = 0 \\ &\rightarrow 0, \quad \text{when } \mu = 1, 2, 3 \end{aligned} \quad (5.15)$$

Therefore, using Eqs. (5.9) and (5.15), we can write the  $S$  matrix as:

$$S = i2\pi\delta(\Delta_{fi} - E_e - E_\nu)G \int d\vec{x} e^{-i\vec{q} \cdot \vec{x}} \phi_p^\dagger(\vec{x}) \mathbb{1} \phi_n(\vec{x}) \bar{u}_e \gamma^0 u_\nu, \quad (5.16)$$

where  $\Delta_{fi} = E_i^n - E_f^p$  is the available energy for the decay and  $\vec{q} = \vec{k} + \vec{k}'$ . Since  $|\vec{q}|$  is of the order of a few MeV and  $|\vec{x}|$  is of the order of the nuclear radius, that is, a few Fermi, the

product  $|\vec{q} \cdot \vec{x}|$  is of the order of  $10^{-2}$  ( $\hbar c = 197$  MeV-fm). Thus, the exponent in Eq. (5.16) can be expanded in powers of  $\vec{q} \cdot \vec{x}$ , that is,

$$e^{-i\vec{q} \cdot \vec{x}} = 1 + (-i\vec{q} \cdot \vec{x}) + \frac{(-i\vec{q} \cdot \vec{x})^2}{2!} + \dots \quad (5.17)$$

Writing  $\phi_p^\dagger \mathbb{1} \phi_n = \phi^\dagger \tau^+ \phi$ , where  $\tau^+$  is the isospin raising operator, that is,  $\tau^+ = \frac{\tau_x + i\tau_y}{2}$ , and  $\phi = \begin{pmatrix} \phi_p \\ \phi_n \end{pmatrix}$ , is a two-component isospinor, the S matrix is written as:

$$S = \pm i 2\pi \delta(\Delta_{fi} - E_e - E_\nu) G \times \int d\vec{x} \left( 1 + (-i\vec{q} \cdot \vec{x}) + \frac{(-i\vec{q} \cdot \vec{x})^2}{2!} + \dots \right) \phi^\dagger(x) \mathbb{1} \tau^+ \phi(x) \bar{u}_e \gamma^0 u_\nu. \quad (5.18)$$

Taking the matrix element of the S matrix in the initial and final states and retaining only the first term in the expansion, we get

$$\langle f | S | i \rangle = S_{fi} = i 2\pi \delta(\Delta_{if} - E_e - E_\nu) G \mathcal{M}_{fi} \quad (5.19)$$

with

$$\mathcal{M}_{fi} = \bar{u}_e \gamma^0 u_\nu \mathcal{M}_F, \text{ where } \mathcal{M}_F = \langle f | \mathbb{1} \tau^+ | i \rangle.$$

It can be seen that in the Fermi theory, the transition operator in the nuclear space is  $\mathbb{1} \tau^+$ , that is, it becomes independent of  $\vec{x}$  and does not induce any change in the spin ( $\vec{S}$ ) or the angular momentum ( $\vec{L}$ ) implying no change in parity. Therefore, the operator describes the nuclear  $\beta$ -decays known as the allowed Fermi transitions corresponding to  $\Delta J = 0$  with no change in the parity. It should be noted that transition operators which include the higher order terms in  $\vec{q} \cdot \vec{x}$  in the expansion (Eq. (5.17)) are called forbidden transitions with decay rates smaller by many orders of magnitude due to  $|\vec{q} \cdot \vec{x}| \approx 10^{-2}$ .

The decay probability per unit time  $d\Gamma$  for a process like:

$$^{14}\text{O}(0^+) \rightarrow ^{14}\text{N}^*(0^+) + e^+ + \nu_e, \quad (5.20)$$

that undergoes Fermi transition, is then derived using the aforementioned S matrix elements  $S_{fi}$  with the general expression of the decay probability per unit time  $d\Gamma = \frac{|S_{fi}|^2}{T}$  integrated over the available phase space (see Section 5.4 for details), that is,

$$d\Gamma = \frac{1}{T} \sum_i \sum_f |S_{fi}|^2 \frac{d\vec{k}}{(2\pi)^3 (2E_e)} \frac{d\vec{k}'}{(2\pi)^3 2E_\nu} \quad (5.21)$$

$$= G^2 \frac{\delta(\Delta_{fi} - E_e - E_\nu)}{(2\pi)^5 2E_e 2E_\nu} \sum_i \sum_f |\mathcal{M}_{fi}|^2 d\vec{k} d\vec{k}', \quad (5.22)$$

where

$$\mathcal{M}_{fi} = \bar{u}_e \gamma^0 u_\nu \mathcal{M}_F \text{ with } \mathcal{M}_F = \langle f | \mathbb{1} \tau^+ | i \rangle, \quad (5.23)$$

leading to

$$\overline{\sum} \sum |\mathcal{M}_{fi}|^2 = 4 |\mathcal{M}_F|^2 E_e E_\nu (1 + \beta_e \cos \theta_{ev}), \quad \beta_e = \frac{|\vec{k}'|}{E_e}, \cos \theta_{ev} = \hat{k}' \cdot \hat{k}. \quad (5.24)$$

Performing the integration over all the neutrino variables assuming neutrinos to be massless, we find:

$$d\Gamma = \frac{G^2}{8\pi^4} |\mathcal{M}_F|^2 E_e |\vec{k}'| (\Delta_{fi} - E_e)^2 dE_e d\Omega_e (1 + \beta_e \cos \theta_{ev})$$

and integrating over the electron angle, we get

$$\frac{d\Gamma}{dE_e} = \frac{G^2}{2\pi^3} |\mathcal{M}_F|^2 E_e |\vec{k}'| (\Delta_{fi} - E_e)^2. \quad (5.25)$$

Integrating over the electron's energy and using the limit  $m_e \rightarrow 0$ , we obtain:

$$\Gamma = \frac{G^2 \Delta_{fi}^5}{60\pi^3} |\mathcal{M}_F|^2. \quad (5.26)$$

In deriving the aforementioned equations, we have assumed the electron and the neutrino to be free particles and represented them by plane waves. While this is true for neutrinos, it is not true for electrons as they move in the Coulomb field of the nucleus. Therefore, instead of a plane wave, the electron wave function should be obtained by solving a relativistic Dirac equation for the continuum states of electrons moving in the Coulomb field of the nucleus  $A(Z, N)$  undergoing  $\beta$ -decay. This is done by treating the nucleus  $A(Z, N)$  as a point nucleus with charge  $Ze$ . It results in multiplying the decay probability/ time,  $d\Gamma$  by a factor known as the Fermi function [224]:

$$F(Z, E_e) = |\psi_{e,Z}(x)|^2 / |\psi_{e,Z}(0)|^2 \quad (5.27)$$

given by:

$$|\psi_{e,Z}(x)|^2 / |\psi_{e,Z}(0)|^2 = 2(1 + \gamma) (2|\vec{k}'||x|)^{-2(1-\gamma)} \exp(\pi Z\alpha E / |\vec{k}'|) \frac{|\Gamma(\gamma \pm iZ\alpha E / |\vec{k}'|)|^2}{|\Gamma(2\gamma + 1)|^2}, \quad (5.28)$$

where  $\gamma = (1 - Z^2\alpha^2)^{\frac{1}{2}}$ ,  $\eta = Z\alpha$  and  $\Gamma$  is the gamma function. The aforementioned expression diverges at  $x = 0$  and is therefore evaluated at  $x = R$ , where  $R$  is the nuclear radius. However, in a realistic situation, the nucleus is taken to have a charge distribution rather than a point nucleus and the Dirac equation is solved numerically. Following this method, the Coulomb correction is obtained and the Fermi function is tabulated to be used in the study of nuclear  $\beta$ -decays.

Performing integration over electron angles, we obtain the expression for the energy distribution of the electron as:

$$\frac{d\Gamma}{dE_e} = \frac{G^2}{2\pi^3} \zeta |\vec{k}'| E_e (\Delta_{fi} - E_e)^2, \quad \text{where } \zeta = |\mathcal{M}_F|^2. \quad (5.29)$$

Integrating over electron's energy, the total decay rate  $\Gamma$  is calculated as:

$$\Gamma = \frac{G^2}{2\pi^3} \zeta f_0(Z, \Delta_{fi}), \quad (5.30)$$

where

$$f_0(Z, \Delta_{fi}) = \int_{E_e=m_e}^{\Delta_{fi}} F(Z, E_e) |\vec{k}'| E_e (\Delta_{fi} - E_e)^2 dE_e, \quad (5.31)$$

where  $f_0(Z, \Delta)$  is called the Fermi integral. The mean life  $\tau = \frac{1}{\Gamma}$  is then defined as:

$$\tau = \frac{1}{\Gamma} = \frac{2\pi^3}{G^2} \frac{1}{\zeta f_0} \quad (5.32)$$

$$\text{and the half life } t_{\frac{1}{2}} = \tau \ln 2. \quad (5.33)$$

The nuclear  $\beta$ -decays are generally characterized by their half life  $t_{\frac{1}{2}}$  represented by a number called  $ft$  value. The value is defined as:

$$ft = \frac{2\pi^3 \ln 2}{G^2 \zeta}, \text{ where } ft = f_0 \times t_{\frac{1}{2}}. \quad (5.34)$$

The  $ft$  values for some of the super-allowed Fermi decays are listed in Table 5.1. When the effect of the Coulomb interaction of the electron with the final nucleus is neglected, while the mass of the electron is retained, we obtain the following expression for the total decay rate  $\Gamma$ :

$$\Gamma = \frac{|\mathcal{M}_F|^2 G^2}{2\pi^3} f_0, \quad (5.35)$$

$$\text{where } f_0 = \frac{d^3}{30} (\Delta_{fi}^2 + 4m_e^2) - \frac{1}{4} d \Delta_{fi}^2 m_e^2 + \frac{1}{4} m_e^4 \Delta_{fi} \ln \left( \frac{\Delta_{fi} + d}{m_e} \right)$$

and  $d = \sqrt{\Delta_{fi}^2 - m_e^2}$ . We see that in the limit of  $m_e \rightarrow 0$ , the equation reduces to Eq. (5.26).

In general, a calculation of the nuclear matrix  $\mathcal{M}_F$  is complicated involving knowledge of the nuclear wave functions. However, in the case of the allowed Fermi transitions corresponding to  $0^+ \rightarrow 0^+$  transitions ( $\beta^+$ -decays), for example,  $^{10}\text{C} \rightarrow ^{10}\text{B}$ ,  $^{14}\text{O} \rightarrow ^{14}\text{N}^*$ ,  $^{34}\text{Cl} \rightarrow ^{34}\text{S}$ ,  $^{42}\text{Sc} \rightarrow ^{42}\text{Ca}$ ,  $^{46}\text{V} \rightarrow ^{46}\text{Ti}$ ,  $^{54}\text{Co} \rightarrow ^{54}\text{Fe}$ , etc., the calculations of the matrix elements are simple. These transitions are between the two members of the isospin triplet states, that is,  $|T=1 \ T_3=\pm 1\rangle$  and  $|T=1 \ T_3=0\rangle$  giving the matrix element

$$\langle T=1 \ T_3=0 | T_- | T=1 \ T_3=1 \rangle = \sqrt{2},$$

such that:

$$\mathcal{M}_F = \sqrt{2}.$$



**Table 5.1**  $ft$  values from super-allowed Fermi decays [225, 226].

Parent	$ft$ (s)
$^{10}\text{C}$	$3078.0 \pm 4.5$
$^{14}\text{O}$	$3071.4 \pm 3.2$
$^{22}\text{Mg}$	$3077.9 \pm 7.3$
$^{26m}\text{Al}$	$3072.9 \pm 1.0$
$^{34}\text{Cl}$	$3070.7 \pm 1.8$
$^{34}\text{Ar}$	$3065.6 \pm 8.4$
$^{38m}\text{K}$	$3071.6 \pm 2.0$
$^{38}\text{Ca}$	$3076.4 \pm 7.2$
$^{42}\text{Sc}$	$3072.4 \pm 2.3$
$^{46}\text{V}$	$3074.1 \pm 2.0$
$^{50}\text{Mn}$	$3071.2 \pm 2.1$
$^{54}\text{Co}$	$3069.8 \pm 2.6$
$^{62}\text{Ga}$	$3071.5 \pm 6.7$
$^{74}\text{Rb}$	$3076.0 \pm 11.0$

Using this value for  $\mathcal{M}_F$ , the experimental values of nuclear energy difference  $\Delta_{fi}$ , and the  $ft$  values given in Table 5.1, the coupling constant  $G$  is evaluated. Using this information, we find  $G = 1.166 \times 10^{-5} \text{ GeV}^{-2}$ .

In addition to the allowed Fermi transitions, nuclear  $\beta$ -decays were also observed where the angular momentum  $J$  of the initial nucleus is changed by one unit, that is,  $\Delta J = 1$  without any change in parity. There are many examples of such decays, some of which are listed in Table 5.2. The Hamiltonian density to describe such decays must have  $\vec{J}(= \vec{L} + \vec{S})$  dependent operators in the non-relativistic limit to allow for the change of  $\vec{J}$  of the initial nucleus without any change in parity, that is, the spin ( $\vec{S}$ ) dependent operators. Therefore, Gamow and Teller [26] proposed the Hamiltonian density to be a scalar product of axial vector currents in the hadronic and leptonic sectors to explain such decays.

$$\mathcal{H}_{\text{int}}^{\text{GT}}(x) = G_A \bar{\psi}_p(x) \gamma^\mu \gamma_5 \psi_n(x) \bar{\psi}_e(x) \gamma_\mu \gamma_5 \psi_\nu(x) + h.c., \quad (5.36)$$

Performing a non-relativistic reduction of the nucleonic current  $J_h^\mu(x) = \bar{\psi}_p(x) \gamma^\mu \gamma_5 \psi_n(x)$ , using Eq. (5.4), we obtain:

$$\bar{\psi}_p(\vec{x}) \gamma^\mu \gamma_5 \psi_n(\vec{x}) \rightarrow 0 \quad i = 0 \quad (5.37)$$

$$\begin{aligned} &\rightarrow \phi^\dagger(\vec{x}) \sigma^i \phi(\vec{x}) \quad i = 1, 2, 3 \\ &= \phi^\dagger(\vec{x}) \vec{\sigma} \tau^+ \phi, \end{aligned} \quad (5.38)$$

leading to the matrix element  $\mathcal{M}_{fi}$  corresponding to the Gamow–Teller transitions as

$$\mathcal{M}_{fi}^{\text{GT}} = \langle f | \vec{\sigma} \tau^+ | i \rangle \bar{u}_e(k') \gamma^i \gamma_5 u_\nu(k) = \mathcal{M}_{GT} \bar{u}(k') \gamma^i \gamma_5 u(k), \quad (5.39)$$

**Table 5.2** The columns list the parent nucleus in the transition, the initial, and final spins, and the transition type. F stands for a pure Fermi transition and GT stands for a Gamow–Teller transition [225, 226].

Parent	$J_i$	$J_f$	Type	Reference
${}^6\text{He}$	0	1	$GT/\beta^-$	[227]
${}^{32}\text{Ar}$	0	0	$F/\beta^+$	[228]
${}^{38m}\text{K}$	0	0	$F/\beta^+$	[229]
${}^{60}\text{Co}$	5	4	$GT/\beta^-$	[230]
${}^{67}\text{Cu}$	3/2	5/2	$GT/\beta^-$	[231]
${}^{114}\text{In}$	1	0	$GT/\beta^-$	[232]
${}^{14}\text{O}/{}^{10}\text{C}$			$F\text{-}GT/\beta^+$	[233]
${}^{26}\text{Al}/{}^{30}\text{P}$			$F\text{-}GT/\beta^+$	[234]

where

$$\mathcal{M}_{GT} = \langle f | \vec{\sigma} \tau^+ | i \rangle. \quad (5.40)$$

The presence of the Pauli spin operator  $\vec{\sigma}$  in  $\mathcal{M}_{GT}$  describes the change in spin of the nucleus by one unit that does not affect the orbital angular momentum state implying no change in parity, that is,  $|\Delta J| = 0, 1$ , with no  $0^+ \rightarrow 0^+$  transition. These transitions are called allowed Gamow–Teller (GT)  $\beta$ -transitions. A calculation of  $\overline{\sum} \sum |\mathcal{M}_{fi}^{GT}|^2$ , from Eq. (5.39) gives:

$$\overline{\sum} \sum |\mathcal{M}_{fi}^{GT}|^2 = 4 |\mathcal{M}_{GT}|^2 E_e E_\nu \left(1 - \frac{1}{3} \beta_e \cos \theta\right),$$

where  $\mathcal{M}_{GT}$  is given by Eq. (5.40) and  $|\mathcal{M}_{GT}|^2 = \langle \sigma \rangle^2$

After integrating over the neutrino variables, the expressions for the energy and angular distribution of the electrons emitted in Gamow–Teller  $\beta$ -decays are obtained as:

$$\begin{aligned} \frac{d\Gamma}{dE_e d\Omega_e} &= \frac{G_A^2}{8\pi^4} |\mathcal{M}_{GT}|^2 |\vec{k}'| E_e (\Delta_{fi} - E_e)^2 \left(1 - \frac{1}{3} \beta_e \cos \theta_{ev}\right), \\ \frac{d\Gamma}{dE_e} &= \frac{G_A^2}{2\pi^3} |\mathcal{M}_{GT}|^2 |\vec{k}'| E_e (\Delta_{fi} - E_e)^2, \end{aligned} \quad (5.41)$$

and the decay rate  $\Gamma$  is given by:

$$\Gamma = \frac{G_A^2}{2\pi^3} f_0 \xi, \quad (5.42)$$

with  $\xi = |\mathcal{M}_{GT}|^2$  and  $f_0$  given in Eq. (5.31). A comparison with the experimental results on the decay rate gives a value of  $G_A = 1.2723(23)G$  [235]. We see that the energy distribution of the electron and the total decay rate are the same in the case of allowed Fermi and allowed GT transitions. Moreover, the energy distribution of electrons in both types of transitions are consistent with the observation that  $m_{\nu_e} = 0$  (Fig. 1.4).

However, many of the nuclear  $\beta$ -decays are of mixed type, that is, they have both the allowed Fermi and GT transitions. The most studied decays of such type are the  $\beta$ -decays of the neutron and  ${}^3_1\text{H}$ , that is,

$$n \rightarrow p + e^- + \bar{\nu}_e, \quad (5.43)$$

$${}^3_1\text{H} \rightarrow {}^3_2\text{He} + e^- + \bar{\nu}_e, \quad (5.44)$$

which involve  $(\frac{1}{2})^+ \rightarrow (\frac{1}{2})^+$  transitions resulting in  $\Delta J = 0$ ,  $|\Delta J| = 1$  with no change in parity corresponding to the allowed Fermi and GT transitions. Some examples of such types of the nuclear transitions are listed in Table 5.2. Before these decays are discussed we describe the general form of the  $\beta$ -decay Hamiltonian density in the next section.

## 5.2.2 General form of the Hamiltonian and the parity violation in $\beta$ -decays

We have seen in the earlier sections that the  $H_{\text{int}}^{\text{Fermi}}(x)$  for the Fermi theory is a scalar product of two vector currents in the nucleon and electron sector (VV) while the  $H_{\text{int}}^{\text{GT}}(x)$  for the GT theory is a scalar product of the two axial vector currents (AA). It was proposed by Gamow and Teller [26], and Bethe and Bacher [27] that, in general, the interaction Hamiltonian could be a sum of a scalar product of all the bilinear covariants, that is, scalar (S), vector (V), pseudoscalar (P), axial vector (A), and tensor (T) which can be formed from the nucleon and lepton fields. Therefore, the general form of the Hamiltonian density for the  $\beta$ -decay interaction can be written as:

$$\mathcal{H}_{\text{int}}^{\beta \text{ decay}}(x) = G \sum_{i=S,V,T,A,P} C_i \bar{\psi}_p(x) O^i \psi_n(x) \bar{\psi}_e(x) O_i \psi_\nu(x) + h.c., \quad (5.45)$$

where  $O^i = 1, \gamma^\mu, \gamma^\mu \gamma_5, \gamma_5, \sigma^{\mu\nu}$  for the scalar (S), vector (V), axial vector (A), pseudoscalar (P), and tensor (T) interactions, respectively and  $C_i$ s are the coupling strengths of these interactions, which could be complex quantities. There would be, thus, five complex or ten real parameters needed to describe the  $\beta$ -decay interaction which should then be determined on the basis of various experimental results obtained in the study of  $\beta$ -decays of nuclei and other elementary particles. The transition operators for describing the nuclear  $\beta$ -decays corresponding to each bilinear term in the interaction Hamiltonian density given in Eq. (5.45), is obtained by taking the non-relativistic limit of the bilinear covariants for which the results are given in Table 5.3 (Appendix A). We observe from Table 5.3 that nuclear  $\beta$ -decays do not provide any information about pseudoscalar interactions while the scalar and vector interactions both describe the Fermi transitions. The axial vector and the tensor interactions describe the Gamow–Teller transitions. The knowledge of the nuclear structure (wave functions), therefore, does not give any information to distinguish between scalar and vector interactions in the case of Fermi transitions or between the axial vector and the tensor interactions in the case of GT transitions. It is only the structure of the leptonic part which would lead to different values for various observables in the nuclear  $\beta$ -decays due to scalar and vector interactions in the case of Fermi transitions and due to the axial vector and tensor interaction in the case of GT transitions.

**Table 5.3** Nucleon operators for the decay  $n \rightarrow p e^- \bar{\nu}_e$  in the relativistic and non-relativistic limits, where  $\sigma_{\mu\nu} = \frac{i}{2}[\gamma_\mu, \gamma_\nu]$ , and  $\psi$ s are the nuclear wave functions.

Coupling	Relativistic limit	Non-relativistic limit
Pseudoscalar (P)	$\bar{\psi}(x)\gamma_5\psi(x)$	0
Scalar (S)	$\bar{\psi}(x)\psi(x)$	$1 \tau^+$
Vector (V)	$\bar{\psi}(x)\gamma_\mu\psi(x)$	$\begin{cases} 1; & \text{for } \mu = 0, \\ 0; & \text{for } \mu = i \end{cases}$
Axial vector (A)	$\bar{\psi}(x)\gamma_\mu\gamma_5\psi(x)$	$\begin{cases} 0; & \text{for } \mu = 0, \\ \sigma_i\tau^+; & \text{for } \mu = i \end{cases}$
Tensor (T)	$\bar{\psi}(x)\sigma_{\mu\nu}\psi(x)$	$\begin{cases} 0; & \text{for } \mu = 0, \nu = 0, \\ \epsilon_{ijk}\sigma^k & \text{for } \mu = i, \nu = j \end{cases}$

The various experiments performed to determine the coupling constants  $C_V$ ,  $C_A$ ,  $C_S$ , and  $C_T$  (Eq. (5.45)) often led to conflicting conclusions in the beginning. The early experiments seemed to prefer the S, T combination, even though there were many experiments favoring the V, A combination.

It took more than 20 years before a clear picture started to emerge for a phenomenological theory of  $\beta$ -decays and weak interactions. The real breakthrough came in 1957 after the discovery of the parity violation in weak processes [33], which was implied by the resolution of the  $\tau - \theta$  puzzle encountered in the study of weak decays of the K mesons in the two and three pion modes. The solution of the puzzle indicated that parity may not be conserved in weak interactions.

There were two particles  $\tau$  and  $\theta$  discovered experimentally with almost the same mass and lifetime decaying respectively into two and three pions in the S-wave state [39]. This implied parity violation if  $\tau$  and  $\theta$  were the same particles, because two pions and three pions in an S-wave will have opposite parities due to the pseudoscalar nature of pions. In view of this suggestion, Lee and Yang [31, 32] analyzed many weak processes and concluded that there was no experimental evidence to contradict the assumption of parity violation in weak interactions. They suggested specific experiments to test this possibility by measuring specific correlation observables in  $\beta$ -decays of nuclei and other weak decays of elementary particles which were parity violating (i.e., changing sign under the transformation  $\vec{r} \rightarrow -\vec{r}$ ) like  $\vec{\sigma}_N \cdot \hat{p}_e$  or  $\vec{\sigma}_e \cdot \hat{p}_e$ , where  $\hat{p}_e$  is the unit vector along the electron momentum and  $\vec{\sigma}_N$  and  $\vec{\sigma}_e$  are, respectively, the nucleon and electron spin operators. The first experiment to test the parity violation in  $\beta$ -decay was performed by Wu et al. [33] with a polarized cobalt nucleus, where a large asymmetry of  $\beta$ -electrons with respect to the spin direction of the polarized  $^{60}\text{Co}$  was observed. In this experiment, a  $^{60}\text{Co}$  ( $J = 5$ ) nucleus undergoes  $\beta$ -decay to  $^{60}\text{Ni}^*$  ( $J = 4$ ) along with an electron and an antineutrino (see Figure 5.3(a)):

$$^{60}\text{Co}(J = 5) \longrightarrow ^{60}\text{Ni}^*(J = 4) + e^-(J = \frac{1}{2}) + \bar{\nu}_e(J = \frac{1}{2}). \quad (5.46)$$

An observation of the nonzero parity violating spin correlation like  $\langle \vec{J}_N \cdot \vec{p}_e \rangle$ , where  $\vec{J}_N$  is the total angular momentum of the nucleus and  $\vec{p}_e$  is the momentum of the emitted electron in

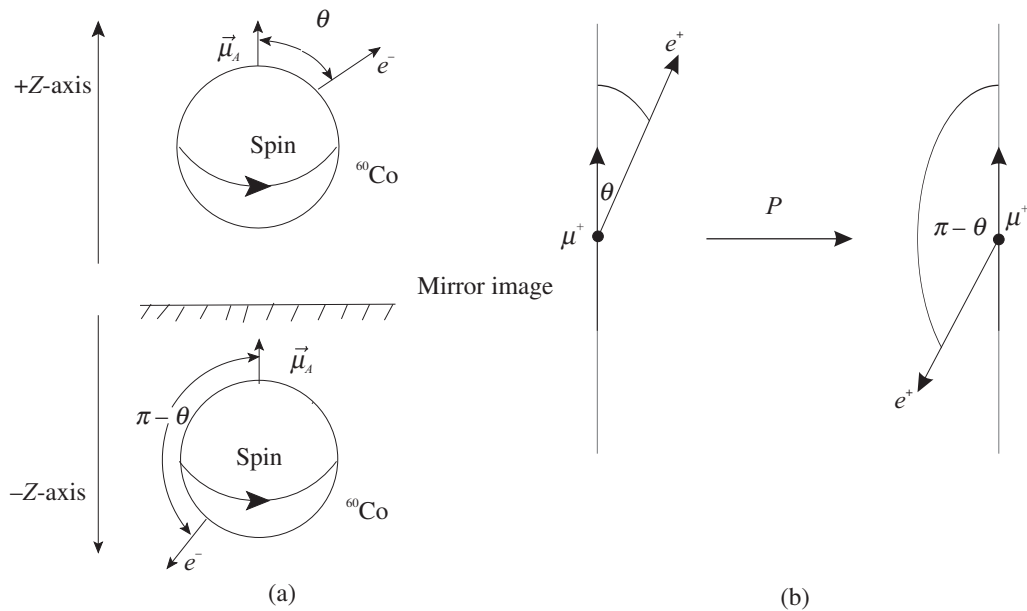


**Figure 5.3** (a) Effect of parity transformation on the process  $^{60}\text{Co} \rightarrow ^{60}\text{Ni}^* + e^- + \bar{\nu}_e$ . The electrons coming at  $\pi - \theta$  direction with respect to the nuclear spin were not observed leading to front-back asymmetry; hence, indication of parity violation in weak interactions. (b) Parity transformation of a muon decaying into a positron.

$\beta$ -decay demonstrated that parity is violated in weak interactions. The direction of the nuclear angular momentum was determined by putting the nucleus in a magnetic field which aligns the angular momentum along the direction of the magnetic field. The direction of the magnetic field was reversed to change the alignment of the angular momentum. The number of electrons were measured in both cases and a nonzero asymmetry was measured.

Around the same time, the observation of a large asymmetry in the emission of positron in the decay of polarized muon confirmed the phenomenon of parity violation in weak processes other than nuclear  $\beta$ -decays [236, 237] as illustrated in Figure 5.3(b). Later on, many experiments on the observable  $\langle \vec{\sigma}_e \cdot \hat{p}_e \rangle$ , that is, the longitudinal polarization of the electrons in the nuclear  $\beta^-$ -decays and the positrons in the nuclear  $\beta^+$ -decays were conducted and the violation of parity in weak interactions was firmly established [34, 35]. The intervening years between 1934 and 1957 were filled with experimental and theoretical activities in the study of weak interaction processes. All the activities made valuable contributions toward the understanding of the physics of weak interactions.

In the presence of parity violation, the interaction Hamiltonian  $\mathcal{H}_{\text{int}}^{\beta \text{ decay}}(x)$  would be a mixture of scalar and pseudoscalar products of the two weak currents, that is, the leptonic and the hadronic currents and can be written, without loss of generality, in the form

$$\mathcal{H}_{\text{int}}^{\beta \text{ decay}}(x) = \sum_{i=S,T,V,A,P} G \bar{\psi}_p(x) O^i \psi_n(x) \bar{\psi}_e(x) O_i (C_i + C'_i \gamma_5) \psi_\nu(x) + \text{h.c.} \quad (5.47)$$

This would involve 10 complex or 20 real parameters  $C_i$  and  $C'_i$  ( $i = S, T, V, A, P$ ) to completely specify the weak interaction Hamiltonian density. Considering this interaction Hamiltonian and following the procedure of non-relativistic reduction of the nucleon wave functions, we write a general form for the matrix element for nuclear  $\beta$ -decays as:

$$\begin{aligned} \mathcal{M}_{fi} = & G \langle f | \sum_i \tau^+ \mathbb{1} | i \rangle \left[ \bar{u}_e (C_S + C'_S \gamma_5) u_\nu + \bar{u}_e \gamma^0 (C_V + C'_V \gamma_5) u_\nu \right] \\ & + G \langle f | \sum_i \vec{\sigma} \tau^+ | i \rangle \left[ \bar{u}_e \vec{\sigma} \gamma^0 (C_A + C'_A \gamma_5) u_\nu + \bar{u}_e \vec{\sigma} (C_T + C'_T \gamma_5) u_\nu \right], \quad (5.48) \end{aligned}$$

where  $\langle f | \sum_i \tau^+ \mathbb{1} | i \rangle = \mathcal{M}_F$  and  $\langle f | \sum_i \vec{\sigma} \tau^+ | i \rangle = \mathcal{M}_{GT}$ . In general, the Fermi transitions could be due to scalar or/and vector interactions. Similarly, the GT interactions could be due to axial vector or/and tensor terms depending upon the values of the constants  $C_i, C'_i$  ( $i = S, T, V, A$ ). However, in a mixed decay like  $\beta$ -decays of  $n$  or  ${}^3\text{H}$ , all the four interactions could contribute. The correct form of the Hamiltonian density was obtained by experimentally determining the constants  $C_i$  and  $C'_i$  ( $i = S, T, V, A$ ) in a phenomenological analysis using the data from the various experiments performed on nuclear  $\beta$ -decays by studying the following observables:

- The energy and angular distributions of electrons (positrons) in the  $\beta$ -decay of unpolarized nuclei.
- The longitudinal polarization of electrons (positrons) from  $\beta$ -decay of the unpolarized nuclei.
- Helicity of the neutrino.
- The spin-momentum correlation like  $\langle \vec{J} \cdot \vec{p}_e \rangle$  and  $\langle \vec{J} \cdot \vec{p}_\nu \rangle$ , where  $\vec{J}$  is the spin of the polarized nucleus,  $\vec{p}_e$  is the momentum of the electron (positron), and  $\vec{p}_\nu$  is the momentum of the antineutrino (neutrino) in the  $\beta^-$  ( $\beta^+$ )-decays of polarized nuclei.

In the following sections, we discuss briefly the conclusions drawn from the study of these observables from various experiments in nuclear  $\beta$ -decays.

### 5.2.3 The energy and angular distribution of electrons (positrons) for the $\beta^+$ ( $\beta^-$ )-decay of unpolarized nuclei

A general calculation of the electron (positron) spectrum following the methods outlined in Section 5.2.1 using the matrix elements given in Eq. (5.48) yields the following result for the energy and angular distributions of electrons (positrons) for the  $\beta$ -decay of unpolarized nuclei  $\beta^-$  ( $\beta^+$ ) decay as [238, 239, 240, 241]:

$$\frac{d\Gamma}{dE_e d\Omega_e} = G^2 F(Z, E_e) \frac{p_e E_e (\Delta_{fi} - E_e)^2}{8\pi^4} \cdot K \left( 1 + a \beta_e \cos \theta_{ev} \pm b \frac{m_e}{E_e} \right), \quad (5.49)$$

where  $K = |\mathcal{M}_F|^2 (D_{SS} + D_{VV}) + |\mathcal{M}_{GT}|^2 (D_{TT} + D_{AA}),$

$$\begin{aligned}
Ka &= |\mathcal{M}_F|^2(-D_{SS} + D_{VV}) + \frac{1}{3}|\mathcal{M}_{GT}|^2(D_{TT} - D_{AA}), \\
Kb &= |\mathcal{M}_F|^2 2\text{Re}(D_{SV}) + |\mathcal{M}_{GT}|^2 2\text{Re}(D_{TA}), \\
\text{and } D_{ij} &= C_i C_j^* + C_i' C_j'^* \quad \text{for } i, j = S, V, T, A.
\end{aligned} \tag{5.50}$$

Integrating over the solid angle, the energy distribution is obtained as:

$$\frac{d\Gamma}{dE_e} = G^2 F(Z, E_e) \frac{p_e E_e (\Delta - E_e)^2}{2\pi^3} K \left( 1 \pm b \frac{m_e}{E_e} \right), \tag{5.51}$$

and integrating over the electron's energy, the total decay rate may be obtained as:

$$\Gamma = \int \frac{d\Gamma}{dE_e} dE_e.$$

A comparison with the experimental results on energy (Figure 5.4) and the angular distribution leads to the following conclusions:

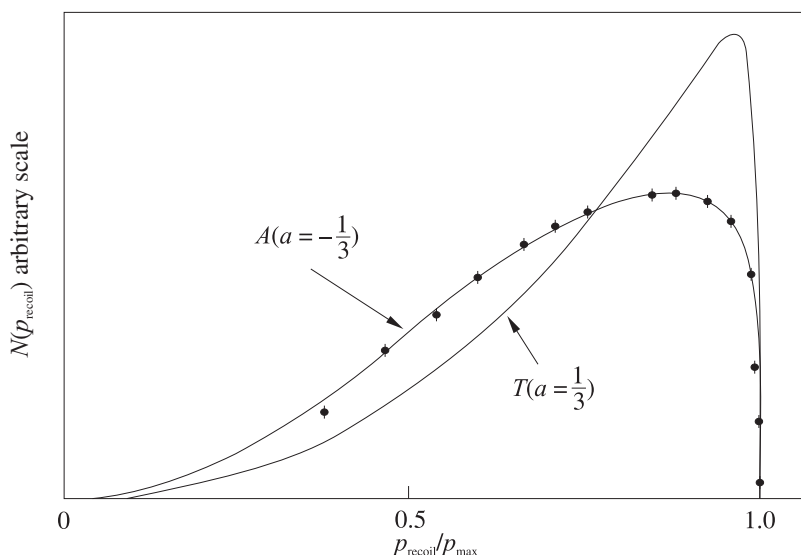


**Figure 5.4** Recoil momentum spectrum for the decay  ${}^6\text{He} \rightarrow {}^6\text{Li} + e^- + \bar{\nu}_e$  together with the predictions for pure A and pure T couplings [242].

1. The energy spectrum can be fitted with a value of  $b = -0.02 \pm 0.09$  for the Fermi transition and  $b = 0.0008 \pm 0.0020$  for the Gamow–Teller transition [243, 244], showing that there is no  $\frac{1}{E}$  dependency in the energy spectrum. This implies that  $D_{SV} = 0$  for the Fermi transition and  $D_{TA} = 0$  for the GT transitions. Assuming the coupling constants  $C_i$ s and  $C_i'$ s to be real (due to T-invariance), this means that the Fermi transitions are either S or V type while GT transitions are either A or T type and there is no interference between them.

2. The endpoint energy of the electron in the energy spectrum shown in Figure 1.4 is  $E_{\max} = 20$  keV. Therefore, it is concluded that mass of the electron neutrino, that is,  $m_{\nu_e}$  is consistent with zero. In fact, in modern times, the very high precision data obtained from the  $\beta$ -decay of  ${}^3\text{H}$  is being used to determine the mass of  $m_{\nu_e}$  with the results that  $m_{\nu_e} < 0.5$  eV (see Section 1.4).
3. The experimental results on the angular distribution of  $e^-(e^+)$  in the  $\beta^-(\beta^+)$  decay of nuclei are consistent with the value  $a = 0.97 \pm 0.14$  [75] for 4 Fermi transitions and  $-0.3343 \pm 0.003$  [227] for GT transitions. These values are close to 1 and  $-\frac{1}{3}$  predicted for the vector interactions in Fermi transitions and the axial vector interactions in GT transitions, respectively (Fig. 5.4).

Therefore, the study of the energy spectrum of electrons (positrons) in nuclear  $\beta^-(\beta^+)$ -decays established that Fermi transitions are due to vector interactions while GT transitions are due to axial vector interactions.

### 5.2.4 The longitudinal polarization of $e^-(e^+)$ from $\beta^-(\beta^+)$ -decays of unpolarized nuclei

The measurement of the longitudinal polarization of electrons (positrons) from the decay of unpolarized nuclei gives additional information about the constants  $C_i$  and  $C'_i$ . The polarization  $P$  of  $e^-(e^+)$  is defined as:

$$P(e^\mp) = \frac{n_R - n_L}{n_R + n_L}, \quad (5.52)$$

where  $n_R$  and  $n_L$  are respectively the number of the right-handed and the left-handed polarizations of  $e^-(e^+)$ . The expression for the polarization  $P(e^\mp)$  is derived to be [238]:

$$P(e^\mp) = \pm\beta \frac{|\mathcal{M}_F|^2(-E_{SS} + E_{VV}) + |\mathcal{M}_{GT}|^2(-E_{TT} + E_{AA})}{|\mathcal{M}_F|^2(D_{SS} + D_{VV}) + |\mathcal{M}_{GT}|^2(D_{TT} + D_{AA})}, \quad (5.53)$$

where the quantities  $E_{ij}$  are defined as:

$$E_{ij} = C_i C_j'^* + C_i' C_j^* \quad (5.54)$$

and  $D_{ij} = C_i C_j^* + C_i' C_j'^*$ . Explicitly, the following results are obtained for  $P(e^\mp)$ :

$$\begin{aligned} P(e^\mp) &= \mp\beta \frac{E_{SS}}{D_{SS}} = \frac{C_S C_S'^* + C_S' C_S^*}{C_S C_S^* + C_S' C_S'^*} \text{ for scalar interaction} \\ &= \pm\beta \frac{E_{VV}}{D_{VV}} = \frac{C_V C_V'^* + C_V' C_V^*}{C_V C_V^* + C_V' C_V'^*} \text{ for vector interaction} \\ &= \mp\beta \frac{E_{TT}}{D_{TT}} = \frac{C_T C_T'^* + C_T' C_T^*}{C_T C_T^* + C_T' C_T'^*} \text{ for tensor interaction} \\ &= \pm\beta \frac{E_{AA}}{D_{AA}} = \frac{C_A C_A'^* + C_A' C_A^*}{C_A C_A^* + C_A' C_A'^*} \text{ for axial vector interaction.} \end{aligned} \quad (5.55)$$



A comparison with the experimental results from the measurements of the polarization of  $e^-(e^+)$  shows that  $P(e^-) = -(0.99 \pm 0.009)\beta$  for the GT decay of  $^{32}\text{P}$  by Brosi et al. [245] which is consistent with  $P(e^\mp) = \mp\beta$  [246, 247].

This implies that in the case of pure Fermi transitions for which  $P(e^-) = -1$ , one has

$$\frac{E_{SS}}{D_{SS}} = 1 \text{ i.e., } |C_S - C_{S'}|^2 = 0 \implies C_S = C_{S'} \text{ for scalar interaction,} \quad (5.56)$$

$$\frac{E_{VV}}{D_{VV}} = -1 \text{ i.e., } |C_V + C_{V'}|^2 = 0 \implies C_V = -C_{V'} \text{ for vector interaction,} \quad (5.57)$$

and in the case of pure GT transition,

$$\frac{E_{TT}}{D_{TT}} = 1 \text{ i.e., } |C_T - C_{T'}|^2 = 0 \implies C_T = C_{T'} \text{ for the tensor interaction,} \quad (5.58)$$

$$\frac{E_{AA}}{D_{AA}} = -1 \text{ i.e., } |C_A + C_{A'}|^2 = 0 \implies C_A = -C_{A'} \text{ for axial vector interaction.} \quad (5.59)$$

From these results, it may be inferred that if the Fermi interaction is a vector interaction then  $C_V = -C_{V'}$ ; and if the GT transition is an axial vector interaction, then  $C_A = -C_{A'}$  with the consequence that for V and A interactions, the  $\mathcal{H}_{\text{int}}(x)$  in Eq. (5.47) can be written as:

$$\mathcal{H}_{\text{int}}(x) = \frac{G_F}{\sqrt{2}} \bar{\psi}_p (C_V \gamma^\mu + C_A \gamma^\mu \gamma^5) \psi_n \bar{\psi}_e \gamma_\mu (1 - \gamma_5) \psi_\nu, \quad G_F = \sqrt{2}G. \quad (5.60)$$

Therefore, the leptonic part in  $\mathcal{H}_{\text{int}}(x)$  is written as:

$$l_\mu = \bar{\psi}_e \gamma_\mu (1 - \gamma_5) \psi_\nu \quad (5.61)$$

implying that  $\psi_\nu$  can be replaced by  $(1 - \gamma_5)\psi_\nu$  in writing the weak interaction Hamiltonian density. Therefore, the Dirac spinor for neutrino  $u_\nu$  enters as  $(1 - \gamma_5)u_\nu$ , that is,  $\nu$  is left-handed. On the other hand, for the S and T interactions, it enters as  $(1 + \gamma_5)u_\nu$ . This leads to the important conclusion that the helicity of the neutrino (antineutrino) is  $-1(+1)$  as discussed in Chapter 2. This was experimentally confirmed by Goldhaber et al. [153] in nuclear  $\beta$ -decays and by Garwin et al. [236] in the case of pion decays.

## 5.2.5 Helicity of the neutrino

The discovery of parity violation and the experimental evidence that neutrino mass is zero, that is,  $m_{\nu_e} = 0$  revived the two-component theory of neutrino. The theory implied that the neutrino (antineutrinos) are left(right)-handed particles or vice versa, as can be seen from the formulation of the two-component theory of neutrino (discussed in Chapter 2). The evidence that neutrinos (antineutrinos) is left (right)-handed was available from the observations made on the longitudinal polarization of the electrons and other spin momentum correlation measurements of the emitted electrons and positrons in many weak decays of nuclei and elementary particles. The helicity of  $\nu_e$  was directly measured in an excellent experiment

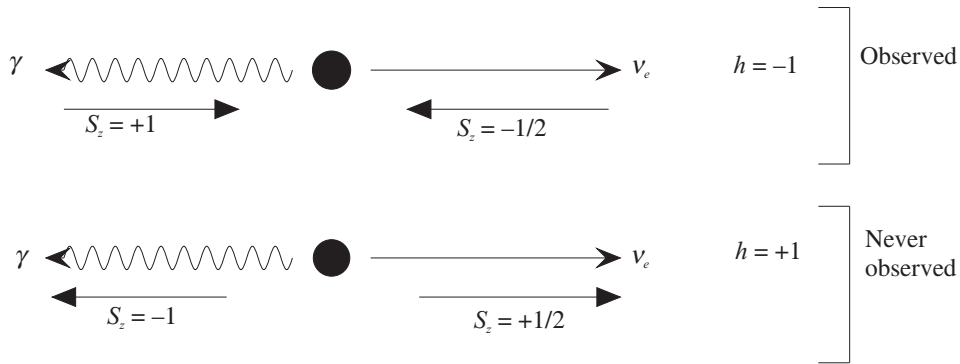
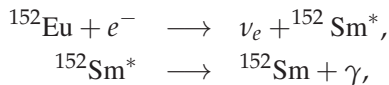


**Figure 5.5** Helicity of neutrino indirectly determined in Goldhaber experiment.

performed by Goldhaber et al. [153]. They measured the polarization of photons in an electron capture experiment using  $^{152}\text{Eu}$  nuclei leading to  $^{152}\text{Sm}^*$  and its radiative decay to  $^{152}\text{Sm}$ .



resulting in the final reaction:



The electron from the K-shell is captured at rest from the  $^{152}\text{Eu}$  nucleus and the momentum conservation requires that  $\vec{p}_{\text{Sm}^*} = -\vec{p}_\nu$ . The emission of photons from  $^{152}\text{Sm}^*$  to the ground state of Sm in the forward direction stops the  $^{152}\text{Sm}$  implying that  $\vec{p}_\gamma = -\vec{p}_{\nu_e}$  in Eq. (5.62), that is, neutrinos and photons are emitted in opposite direction to each other. Hence, if we choose the neutrino direction to be along the Z-axis, then the photon is emitted in the negative Z-direction. The spin considerations (the angular momentum  $J$  of  $^{152}\text{Eu}$  ( $J_i$ ) and  $^{152}\text{Sm}$  ( $J_f$ ) in the initial and the final states being zero, that is,  $J_i = J_f = 0$ ) of initial and final particles in Eq. (5.62) show that the polarization state of the emitted photons determine the helicity of the neutrino. The electron in the K-shell has  $J = \frac{1}{2}$  ( $L = 0, S = \frac{1}{2}$ ) while  $^{152}\text{Eu}$  has  $J = 0$  leading to  $^{152}\text{Sm}^*$  which has  $J = 1$  and decays into  $^{152}\text{Sm}$  with  $J = 0$ . Therefore, the total angular momentum in the initial state is  $\frac{1}{2}$  due to the electron spin and can have  $J_Z = \pm\frac{1}{2}$ . The photon is transverse so it can have only  $S_Z = \pm 1$ . Therefore, if  $J_Z^e = +\frac{1}{2}$ , it can come from  $J_Z^\gamma = +1, S_Z^\nu = -\frac{1}{2}$ , and if  $J_Z^e = -\frac{1}{2}$ , it can come only from  $J_Z = -1, S_Z^\nu = +\frac{1}{2}$  (Figure 5.5). Hence, if the neutrino has negative helicity, that is,  $S_Z^\nu = -\frac{1}{2}$ , then only  $S_Z^\gamma = +1$  is possible. Thus, the polarization state of the photon determines the helicity of the neutrino. If the photon has left-handed polarization, the helicity of the neutrino is  $-1$  and if the photon has right-handed polarization, the neutrino has helicity  $+1$ . In an elegant experiment, Goldhaber et al. [153] measured the circular polarization of photons emitted by Compton scattering in a magnetized iron block and confirmed that the emitted photons were left-handed, thus determining the helicity of  $\nu_e$  conclusively to be  $-1$ .

In later experiments done on the muon capture process using  $^{12}\text{C}$ , that is,



the helicity of  $\nu_\mu$  was determined by measuring the recoil polarization of the final nucleus  $^{12}\text{B}$  in the direction of its recoil momentum. A typical measurement by Roesch et al. [248] found the helicity of  $\nu_\mu$  to be  $-1.00 \pm 0.11$  consistent with negative helicity as predicted theoretically.

Another experiment was performed by Garwin et al. [236], who observed pions decay at rest. Consider the charged pions  $\pi^\pm$  decaying to  $\mu^\pm + \nu_\mu(\bar{\nu}_\mu)$ . The momentum of muons

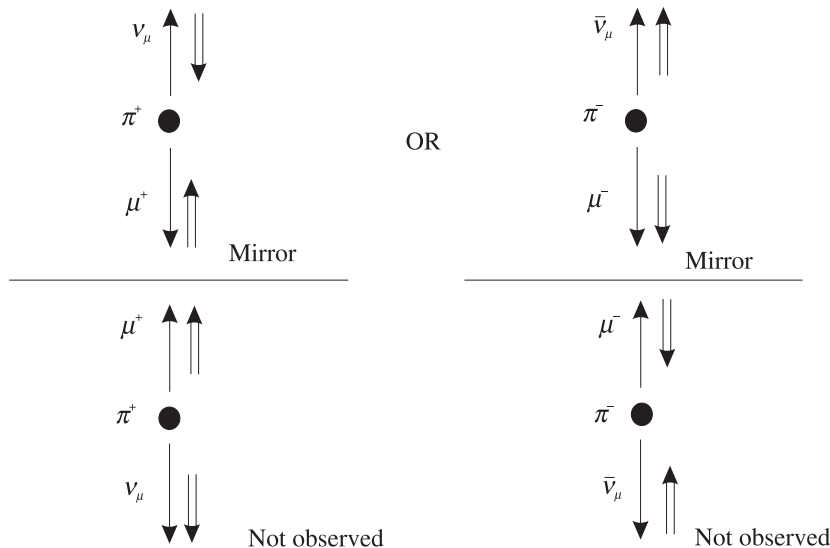


Figure 5.6 Pion decay at rest.

will be opposite in direction to the momentum of neutrinos. To conserve the total angular momentum, their spins should also be oppositely directed (Figure 5.6). We can define the helicity as follows.

$$h = \frac{\vec{\sigma} \cdot \vec{p}}{|\vec{p}|} = +1 \text{ for } \vec{\sigma} \uparrow \uparrow \vec{p} \text{ and } -1 \text{ for } \vec{\sigma} \uparrow \downarrow \vec{p}.$$

The top part of Figure 5.6 would therefore imply  $h = -1(+1)$  for both  $\mu^+$  and  $\nu_\mu$  ( $\mu^-$  and  $\bar{\nu}_\mu$ ). The mirror reflection of this process would be equivalent to parity inversion. In this case,  $h = +1(-1)$  for both  $\mu^+$  and  $\nu_\mu$  ( $\mu^-$  and  $\bar{\nu}_\mu$ ), that is, if parity is conserved, both helicities should be equally probable. However, it was observed from  $\pi^+$  decay that the polarization of  $\mu^+$  is negative and that for  $\pi^-$  decay, the polarization of  $\mu^-$  is positive. Therefore, it was concluded that parity is not conserved in weak interactions. This experiment also provided the evidence that the helicity of  $\nu_\mu$  ( $\bar{\nu}_\mu$ ) coming from  $\pi^+$  ( $\pi^-$ ) decay is negative (positive), that is,  $h = -1(+1)$ , corresponding to upper diagrams in Figure (5.6).

### 5.2.6 Spin-momentum correlations in the $\beta$ -decay of polarized nuclei

In the case of nuclear  $\beta$ -decays of polarized nuclei, the direction of the polarization can be used as a reference direction to measure the angular distribution of electrons (positrons) as was done in the famous experiment of Wu et al. [33]. The asymmetry of the electron (positron) angular distribution is sensitive to the relative sign between  $C_i$  and  $C'_i$  just like the longitudinal polarization of electrons (positrons) in the case of  $\beta$ -decays of unpolarized nuclei. The angular distribution of electrons from the  $\beta$ -decays of a nucleus corresponding to the transition  $J_i \rightarrow J_f$  is given by [238, 239, 240, 241]:

$$\frac{d\Gamma}{d\Omega} \propto \zeta(1 + A\langle\hat{J}_i\rangle \cdot \hat{p}_e), \quad (5.64)$$

where  $\langle\hat{J}_i\rangle$  is the nuclear polarization of the initial nuclear state with spin  $\vec{J}$  and

$$\begin{aligned} \zeta &= |\mathcal{M}_F|^2 D_{VV} + |\mathcal{M}_{GT}|^2 D_{AA}, \\ A\zeta &= \pm \Lambda_{J_i J_f} |\mathcal{M}_{GT}|^2 E_{AA} - 2\delta_{J_i J_f} |\mathcal{M}_F| |\mathcal{M}_{GT}| \sqrt{\frac{J_i}{J_i + 1}} \text{Re}(E_{VA}), \end{aligned} \quad (5.65)$$

where  $+$  ( $-$ ) is for electron (positron) and

$$\Lambda_{J_i J_f} = \begin{cases} -J_i/(J_i + 1) & \text{if } J_f = J_i + 1, \\ 1/(J_i + 1) & \text{if } J_f = J_i \\ 1 & \text{if } J_f = J_i - 1. \end{cases} \quad (5.66)$$

In the case of  $^{60}\text{Co} \rightarrow ^{60}\text{Ni} \ e^- \bar{\nu}_e$  decay, which is a GT transition corresponding to  $J_i = 5 \rightarrow J_f = 4$ ,  $\Lambda_{J_i J_f} = 1$  giving  $A = \frac{E_{AA}}{D_{AA}}$  which was found to be  $-1$  in the case of Wu's experiment. From Eq. (5.59), this implies that  $C_A = -C'_A$ .

### 5.2.7 Mixed $\beta$ -transitions and sign of $\frac{C_A}{C_V}$

We see from Eq. (5.65) that a mixed transition having Fermi as well as Gamow–Teller transitions will give information about the interference term  $E_{VA} = C_V C_A^* + C_V^* C_A$  from an observation of the spin correlation  $A$ . For simplicity, let us consider the case of the polarized free neutron decays which correspond to the  $\beta$ -decay of  $n(\frac{1}{2}^+) \rightarrow p(\frac{1}{2}^+) + e^- + \bar{\nu}_e$ . In this case, the transition rate for the polarized neutron is expressed as [226, 241]:

$$\begin{aligned} d\Gamma(\hat{\sigma}_n, \vec{p}_e, \vec{p}_\nu) &\propto F(E_e) d\Omega_e d\Omega_\nu \left[ 1 + a \frac{\vec{p}_e \cdot \vec{p}_\nu}{E_e E_\nu} + b \frac{m_e}{E_e} \right. \\ &\quad \left. + \langle \vec{\sigma}_n \rangle \cdot \left( A \frac{\vec{p}_e}{E_e} + B \frac{\vec{p}_\nu}{E_\nu} + D \frac{\vec{p}_e \times \vec{p}_\nu}{E_e E_\nu} + R \frac{\vec{\sigma}_e \times \vec{p}_e}{E_e} + \dots \right) \right], \end{aligned} \quad (5.67)$$

**Table 5.4** Values of the coefficients  $A$  and  $B$  appearing in Eq. (5.67).

Coefficient	Value	Year	$\langle m_e/E_e \rangle$	Reference
$A$	$-0.1146(19)$	1986	0.581	[249]
	$-0.1160(9)(12)$	1997	0.582	[250]
	$-0.1135(14)$	1997	0.558	[251]
	$-0.11926(31)(42)$	2013	0.559	[252]
	$-0.12015(34)(63)$	2018	0.586	[253]
	$-0.11869(99)$		0.569	Average (S=2.6)
$B$	$0.9894(83)$	1995	0.554	[254]
	$0.9801(46)$	1998	0.594	[255]
	$0.9670(120)$	2005	0.600	[256]
	$0.9802(50)$	2007	0.598	[257]
	$0.9805(30)$		0.591	Average

where

$$a = \frac{1 - |\lambda|^2}{1 + 3|\lambda|^2}, \quad A = -2 \frac{|\lambda|^2 + \text{Re}\lambda}{1 + 3|\lambda|^2},$$

$$B = 2 \frac{|\lambda|^2 - \text{Re}\lambda}{1 + 3|\lambda|^2}, \quad D = 2 \frac{\text{Im}\lambda}{1 + 3|\lambda|^2},$$

with  $\lambda = \frac{C_A}{C_V}$ .

The term  $D$  represents the measure of T-violation. Assuming T-invariance, we find that  $\lambda = \frac{C_A}{C_V}$  is real and can be obtained by a measurement of the spin correlation of the polarized neutron with momentum of electron ( $\vec{p}_e$ ) or neutrino ( $\vec{p}_\nu$ ), through the measurement of coefficients  $A$  or  $B$ . If both can be measured, we determine  $\text{Re}\lambda$  directly because  $A + B = -\frac{4\text{Re}\lambda}{1+3\lambda^2}$ . The values of  $A$  and  $B$  are given in Table 5.4.

It should be noted that in the case of neutron decay, the decay rate  $\Gamma$  is given by

$$ft = \frac{2\pi^3 \ln 2}{G^2 C_V^2 (1 + 3\lambda^2)}. \quad (5.68)$$

Therefore,  $|\lambda|^2$  is determined from the  $ft$  value as well as from the coefficient  $a (= \frac{1-\lambda^2}{1+3\lambda^2})$  from the angular distribution. Information regarding the spin-momentum correlation measurements have come from the extensive experiments that have been done over the last 20 years at ILL Grenoble [226] using the electron spectrometer PERKEO and also in other experiments. The current value of  $\lambda$  determined from these experiments is given by [117]

$$\lambda = \frac{C_A}{C_V} = -1.2732 \pm 0.0023. \quad (5.69)$$

### 5.3 Two-component Neutrino and the $V - A$ Theory

The study of various observables in the nuclear  $\beta$ -decay like the decay rates, energy and angular distributions of electrons (positrons), their polarizations and spin–momentum correlations with the polarization of the initial nucleus established the following:

1. Neutrinos are almost massless spin  $\frac{1}{2}$  particles.
2. The parity is maximally violated in  $\beta$ -decays.
3. Neutrinos (antineutrinos) have negative (positive) helicity.
4. Fermi transitions are mainly due to vector interactions while Gamow–Teller transitions are mainly due to axial vector transitions.
5. The relative strength of the axial vector and the vector interactions is  $\approx 1.26$ , that is,  $|\frac{C_A}{C_V}| = 1.26$ .
6. The relative sign between the vector and the axial vector interactions is negative, that is,  $\frac{C_A}{C_V} = -1.26$ .

These observations imply that

- i) neutrinos, which can be considered to be massless, can then be described by a two-component theory of massless spin  $\frac{1}{2}$  particles (Chapter 3).
- ii) only the left-handed neutrinos (and the right-handed antineutrinos) couple through lepton currents with vector and axial vector current of hadrons in the  $\beta$ -decay processes through a combination  $V - A$ .

In view of these observations, the two-component theory of massless spin  $\frac{1}{2}$  fermions proposed earlier by Weyl was revived to formulate a theory for weak interactions by Marshak and Sudarshan [41], Feynman and Gell-Mann [42], and Sakurai [43] almost simultaneously, which is known as the  $V - A$  theory of weak interactions. This theory is explained here.

We write the wave function  $\psi_\nu$  of neutrinos as:

$$\psi_\nu = \psi_\nu^L + \psi_\nu^R, \quad (5.70)$$

where  $\psi_\nu^L = \frac{1-\gamma_5}{2}\psi_\nu$  and  $\psi_\nu^R = \frac{1+\gamma_5}{2}\psi_\nu$  are respectively the left-handed and the right-handed components of the neutrino wave functions. Similarly, we write the electron wave function  $\psi_e = \psi_e^L + \psi_e^R$ , where  $\psi_e^L$  is the left-handed electron and  $\psi_e^R$  is the right-handed electron. It is straightforward to see that  $\psi_\nu^L$  couples to  $\psi_e^L$  only through vector (V) and axial vector (A) interactions and not through scalar (S), or tensor (T) interactions, that is,

$$\begin{aligned} C_S \bar{\psi}_e^L \psi_\nu^L &= 0, & (\text{Scalar}) \\ C_T \bar{\psi}_e^L \sigma_{\mu\nu} \psi_\nu^L &= 0, & (\text{Tensor}) \\ C_V \bar{\psi}_e^L \gamma_\mu \psi_\nu^L &= C_V \bar{\psi}_e \gamma_\mu \frac{(1-\gamma_5)}{2} \psi_\nu, & (\text{Vector}) \\ C_A \bar{\psi}_e^L \gamma_\mu \gamma_5 \psi_\nu^L &= C_A \bar{\psi}_e \gamma_\mu \gamma_5 \frac{(1-\gamma_5)}{2} \psi_\nu. & (\text{Axial vector}) \end{aligned} \quad (5.71)$$

Therefore, assuming that only the left-handed components of the lepton fields and the hadron fields couple in the theory of  $\beta$ -decay, we arrive at the  $V - A$  theory of weak interactions.

## 5.4 Weak Interaction of Muon

Muon was discovered in cosmic rays in 1937 [89]; its properties were determined from studies of its weak interaction through its decays, scattering, and capture from nucleons and nuclei. It was established to be a heavy lepton of mass  $m_\mu = 105.658$  MeV with spin  $\frac{1}{2}$  and its own neutrino  $\nu_\mu$  and lepton number  $L_\mu$ . The properties of electrons, muons, and their neutrinos are listed in Table 5.5. The interaction of muons  $\mu$  and their neutrinos  $\nu_\mu$  with matter is described through the following processes:

**Table 5.5** Electron and muon families with their respective lepton numbers [117].

Particle	$L_e$	$L_\mu$	Mass (MeV)	Life time (s)
$\nu_e$	+1	0	$< 2 \times 10^{-6}$	-
$e^-$	+1	0	0.51099	-
$\nu_\mu$	0	+1	$< 0.19$	-
$\mu^-$	0	+1	105.65837	$2.197 \times 10^{-6}$

### 1. Weak decays of muon

$$\mu^- \rightarrow e^- + \bar{\nu}_e + \nu_\mu. \quad (5.72)$$

### 2. Inverse muon-decay and $\nu_\mu$ scattering

$$\nu_\mu + e^- \rightarrow \nu_e + \mu^- \quad \text{and} \quad \nu_e + \mu^- \rightarrow \nu_\mu + e^-. \quad (5.73)$$

### 3. Muon capture from nucleons and nuclei

$$\mu^- + p \rightarrow n + \nu_\mu \quad \text{and} \quad \mu^- + A(Z, N) \rightarrow \nu_\mu + A'(Z - 1, N + 1). \quad (5.74)$$

### 4. Neutrino scattering from nucleons and nuclei

$$\begin{aligned} \nu_\mu + n &\rightarrow \mu^- + p, & \bar{\nu}_\mu + p &\rightarrow \mu^+ + n, \\ \nu_\mu + A(Z, N) &\rightarrow \mu^- + A'(Z + 1, N - 1), \\ \bar{\nu}_\mu + A(Z, N) &\rightarrow \mu^+ + A'(Z - 1, N + 1). \end{aligned} \quad (5.75)$$

In this section, we describe the weak interactions of muons focusing mainly on muon-decay and inverse muon-decay processes for which the Hamiltonian density is described by:

$$\mathcal{H}_{\text{int}}(x) = \frac{G_\mu}{\sqrt{2}} \bar{\psi}_{\nu_\mu} \gamma_\mu (1 - \gamma_5) \psi_\mu \bar{\psi}_{\nu_e} \gamma^\mu (1 - \gamma_5) \psi_e + h.c. \quad (5.76)$$

involving the point interaction of electron and muon currents as shown in Figure 5.7.

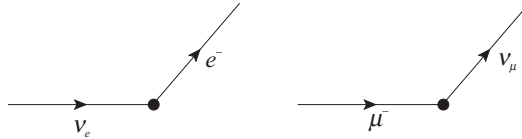


**Figure 5.7** Lepton current connects  $\nu_e$  to  $e^-$  and  $\nu_\mu$  to  $\mu^-$ .

### 5.4.1 Weak decay of muons

The weak decay of the muon

$$\mu^-(p') \rightarrow e^-(p) + \bar{\nu}_e(k) + \nu_\mu(k') \quad (5.77)$$

is diagrammatically shown in Figure 5.8, where  $p'$  and  $k'$  are the momenta of the muon ( $\mu^-$ ) and the muon neutrino ( $\nu_\mu$ ) and  $p$  and  $k$  are the momenta of the electron ( $e^-$ ) and the electron antineutrino ( $\bar{\nu}_e$ ). All the particles in this decay are point particles and therefore, the vertex has no structure (Figure 5.8). The coupling  $G_\mu$  is taken to be constant and is determined using the life time of the muon. Since the emission of the electron in the weak interaction processes

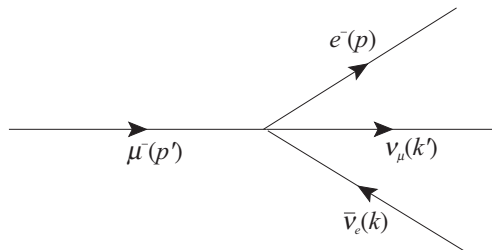


**Figure 5.8** Muon-decay at rest.

is known to be accompanied by an electron type antineutrino ( $\bar{\nu}_e$ ), the other neutral particle was identified as a neutrino associated with a muon, that is, muon neutrino ( $\nu_\mu$ ) and the decay probability per unit time for the initial muon is given as:

$$d\Gamma = \frac{1}{(2\pi)^5 2m_\mu} \frac{d\vec{p}}{2E_e} \frac{d\vec{k}}{2k^0} \frac{d\vec{k}'}{2k'^0} \delta^4(p' + p + k - k') \sum_{s_{\nu_e}, s_{\nu_\mu}} |\mathcal{M}|^2, \quad (5.78)$$

where  $s_{\nu_e}$  and  $s_{\nu_\mu}$  are neutrino spins.



The transition matrix element  $\mathcal{M}$  is given by:

$$\mathcal{M} = \frac{G_\mu}{\sqrt{2}} \left[ \bar{u}_{\nu_\mu}(k', s_{\nu_\mu}) \gamma^\rho (1 - \gamma_5) u_\mu(p', s') \right] \left[ \bar{u}_e(p, s) \gamma_\rho (1 - \gamma_5) u_{\nu_e}(k, s_{\nu_e}) \right].$$

We define

$$\sum_{\text{initial spins}} \sum_{\text{final spins}} |\mathcal{M}|^2 = \frac{G_\mu^2}{2} \mathcal{M}^{\rho\lambda}(\mu) \mathcal{M}_{\rho\lambda}(e),$$

where

$$\mathcal{M}^{\rho\lambda}(\mu) = \mathcal{M}^\rho(\mu) \mathcal{M}^{\lambda\dagger}(\mu) = \sum \left[ \bar{u}_{\nu_\mu} \gamma^\rho (1 - \gamma_5) u_\mu \right] \left[ \bar{u}_{\nu_\mu} \gamma^\lambda (1 - \gamma_5) u_\mu \right]^\dagger,$$

$$\mathcal{M}_{\rho\lambda}(e) = \mathcal{M}_\rho(e) \mathcal{M}_\lambda^\dagger(e) = \sum \left[ \bar{u}_{\nu_e} \gamma_\rho (1 - \gamma_5) u_{\nu_e} \right] \left[ \bar{u}_{\nu_e} \gamma_\lambda (1 - \gamma_5) u_{\nu_e} \right]^\dagger.$$

Considering that the electron and muon are both polarized with spins  $s$  and  $s'$ , respectively, we can write:

$$u_\mu \bar{u}_\mu = (\not{p}' + m_\mu) \left( \frac{1 + \gamma_5 \not{s}'}{2} \right), \quad (5.79)$$

$$u_e \bar{u}_e = (\not{p} + m_e) \left( \frac{1 + \gamma_5 \not{s}}{2} \right), \quad (5.80)$$

$$\begin{aligned} \mathcal{M}^{\rho\lambda}(\mu) &= \frac{1}{2} \text{Tr} \left[ (\not{p}' + m_\mu) (1 + \gamma_5 \not{s}') \gamma^\lambda (1 - \gamma_5) \not{k}' \gamma^\rho (1 - \gamma_5) \right] \\ &= 4 \left\{ (p'^\lambda - m_\mu s'^\lambda) k'^\rho - (p' - m_\mu s') \cdot k' g^{\rho\lambda} \right. \\ &\quad \left. + (p'^\rho - m_\mu s'^\rho) k'^\lambda + i \epsilon^{\alpha\lambda\beta\rho} (p'_\alpha - m_\mu s'_\alpha) k'_\beta \right\}, \end{aligned} \quad (5.81)$$

with similar results for  $\mathcal{M}_{\rho\lambda}(e)$ , with  $p' \rightarrow p$ ,  $s' \rightarrow s$ , and  $m_\mu \rightarrow m_e$ ,  $k' \rightarrow k$  leading to:

$$\sum_{s_{\nu_e}, s_{\nu_\mu}} |\mathcal{M}|^2 = \frac{G_\mu^2}{2} 64 (p' - m_\mu s') \cdot k (p - m_e s) \cdot k', \quad (5.82)$$

where the spin vectors  $s^\mu$  and  $s'^\mu$  are given in the rest frame of muons such that:

$$s'^\mu = (0, \hat{s}'), \quad s^\mu = \left( \frac{\vec{p}_e \cdot \hat{s}}{m_e}, \hat{s} + \frac{(\vec{p}_e \cdot \hat{s}) \vec{p}_e}{m_e(E + m_e)} \right). \quad (5.83)$$

Putting this value of  $|\mathcal{M}|^2$  in Eq. (5.78) we obtain the decay probability of  $d\Gamma$  as:

$$\begin{aligned}
 d\Gamma &= \frac{64 G_\mu^2}{2} \frac{d\vec{p}}{(2\pi)^5} \frac{1}{2E_e 2m_\mu} \int \frac{d\vec{k}}{2E_\nu} \frac{d\vec{k}'}{2E'_\nu} \delta^4(p + k + k' - p') \\
 &\quad (p' - m_\mu s') \cdot k (p - m_e s) \cdot k' \\
 &= \frac{2 G_\mu^2}{(2\pi)^5} \frac{d\vec{p}}{m_\mu E_e} \int \frac{d\vec{k}}{E_\nu E'_\nu} \delta^4(p + k + k' - p') (p' - m_\mu s') \cdot k (p - m_e s) \cdot k' \\
 &= \frac{2 G_\mu^2}{(2\pi)^5} \frac{d\vec{p}}{m_\mu E_e} (p'^\alpha - m_\mu s'^\alpha) (p^\beta - m_e s^\beta) I_{\alpha\beta},
 \end{aligned} \tag{5.84}$$

where

$$I_{\alpha\beta} = \int \frac{d\vec{k}}{E_\nu} \frac{d\vec{k}'}{E'_\nu} \delta^4(k + k' - q) k'_\alpha k_\beta. \tag{5.85}$$

Here,  $q = k - k' = p' - p$  and  $I_{\alpha\beta}$  is a symmetric tensor of rank 2 depending only on momentum  $q_\alpha$ . Therefore, we can write, in the most general form,

$$I_{\alpha\beta} = A q^2 g_{\alpha\beta} + B q_\alpha q_\beta. \tag{5.86}$$

It can be shown using the expression for  $I_{\alpha\beta}$  in Eq. (5.85) that  $A = \frac{\pi}{6}$ ,  $B = \frac{\pi}{3}$  such that  $I_{\alpha\beta} = \frac{\pi}{6} (q^2 g_{\alpha\beta} + 2q_\alpha q_\beta)$  giving

$$d\Gamma = \frac{\pi}{3} \frac{G_\mu^2}{(2\pi)^5} \frac{d\vec{p}}{m_\mu E_e} (p' - m_\mu s')^\alpha (p - m_e s)^\beta (q^2 g_{\alpha\beta} + 2q_\alpha q_\beta). \tag{5.87}$$

Evaluating in the rest frame of muon, where

$$\begin{aligned}
 p^{\alpha'} &= (m_\mu, 0); \quad s^{\alpha'} = (0, \vec{s}'), \\
 p^\beta &= (E_e, \vec{p}_e); \quad s^\beta = \left( \frac{\hat{s} \cdot \vec{p}_e}{m_e}, \hat{s} + \frac{(\vec{p}_e \cdot \hat{s}) \vec{p}_e}{(m_e + E_e)m_e} \right), \\
 q^\alpha &= (m_\mu - E_e, -\vec{p}_e),
 \end{aligned} \tag{5.88}$$

we obtain:

$$\begin{aligned}
 d\Gamma &= \frac{\pi G_\mu^2}{3(2\pi)^5 m_\mu} d\Omega_e |\vec{p}_e| dE_e \left[ (m_\mu^2 + E_e^2 - 2m_\mu E_e - |\vec{p}_e|^2) \right. \\
 &\quad \times \left[ (E_e - \vec{p}_e \cdot \hat{s}) m_\mu + m_\mu \left( \vec{p}_e - m_e \hat{s} - \frac{\vec{p}_e \cdot \hat{s}}{E_e + m_e} \vec{p}_e \right) \cdot \vec{s}' \right] \\
 &\quad + 2 \left( (E_e - \vec{p}_e \cdot \hat{s}) (m_\mu - E_e) + \left( \vec{p}_e - m_e \hat{s} - \frac{\vec{p}_e \cdot \hat{s}}{E_e + m_e} \vec{p}_e \right) \cdot \vec{p}_e \right) \\
 &\quad \times \left. (m_\mu^2 - m_\mu E_e - m_\mu \vec{s}' \cdot \vec{p}_e) \right].
 \end{aligned} \tag{5.89}$$

Since  $m_e \ll m_\mu$ , we may evaluate the decay rate in the extreme relativistic limit for the electron, that is,  $m_e \rightarrow 0$ ,  $|\vec{p}_e| \rightarrow E_e$  and  $\vec{p}_e \rightarrow \hat{n}E_e$ , and obtain:

$$d\Gamma = \frac{\pi G_\mu^2}{3(2\pi)^5 m_\mu} d\Omega_e m_\mu^3 E_e^2 dE_e (1 - \hat{n} \cdot \hat{s}) \left[ \left(3 - \frac{4E_e}{m_\mu}\right) + \left(1 - \frac{4E_e}{m_\mu}\right) \hat{n} \cdot \hat{s}' \right]. \quad (5.90)$$

It can be shown that

$$E_e^{\max} = \frac{m_\mu^2 + m_e^2}{2m_\mu} \simeq \frac{m_\mu}{2} \quad (5.91)$$

$$\text{and } |\vec{p}_e^{\max}| = \frac{m_\mu^2 - m_e^2}{2m_\mu} \simeq \frac{m_\mu}{2}. \quad (5.92)$$

We define a dimensionless variable

$$\epsilon = \frac{E_e}{E_{\max}} = \frac{2E_e}{m_\mu}, \quad (5.93)$$

and write

$$d\Gamma = \frac{G_\mu^2 m_\mu^5}{192\pi^3} 2\epsilon^2 (3 - 2\epsilon) \left( \frac{1 - \hat{n} \cdot \hat{s}}{2} \right) \left[ 1 + \left( \frac{1 - 2\epsilon}{3 - 2\epsilon} \right) \hat{n} \cdot \hat{s}' \right] \frac{d\Omega}{4\pi} d\epsilon. \quad (5.94)$$

This equation gives the angular and energy distributions of the electron, information about the helicity of the emitted electron, as well as the asymmetry in the electron direction with respect to the spin of the muon in case of the decay of the polarized muon. For the spin sum over the final electron and spin average over the muon spin, let us define the spin direction such that  $\hat{n} \cdot \hat{s}' = P \cos \theta$ , where  $P$  is the degree of polarization of the muon and write

$$d\Gamma = \frac{G_\mu^2 m_\mu^5}{192\pi^3} \left( \frac{1 - \hat{n} \cdot \vec{s}}{2} \right) A [1 + B(P \cos \theta)] \frac{d\Omega}{4\pi} d\epsilon, \quad (5.95)$$

where

$$A = 2\epsilon^2 (3 - 2\epsilon) \text{ and } B = \left( \frac{1 - 2\epsilon}{3 - 2\epsilon} \right).$$

In the case of the unpolarized muon, we average over the spin directions of the muon by integrating over the angle  $\theta$  and obtain:

$$d\Gamma = \frac{G_\mu^2 m_\mu^5}{192\pi^3} \left( \frac{1 - \hat{n} \cdot \hat{s}}{2} \right) 2\epsilon^2 [3 - 2\epsilon] d\epsilon. \quad (5.96)$$

### (i) Decay rate

The decay rate for the right-handed electron ( $\hat{n} \cdot \hat{s} = +1$ ) is zero. Taking  $\hat{n} \cdot \hat{s} = -1$ , we obtain:

$$d\Gamma = \frac{G_\mu^2 m_\mu^5}{192\pi^3} 2\epsilon^2 [3 - 2\epsilon] d\epsilon \quad (5.97)$$

leading to the decay rate

$$\Gamma = \frac{G_\mu^2 m_\mu^5}{192\pi^3}. \quad (5.98)$$

Taking into account the electron mass terms in the decay rate which we have neglected, we obtain  $\Gamma = f(m_e)\Gamma(m_e = 0)$ , where

$$\begin{aligned} f(m_e) &= 1 - 8\frac{m_e^2}{m_\mu^2} + 8\frac{m_e^4}{m_\mu^4} - \frac{m_e^8}{m_\mu^8} - 12\frac{m_e^4}{m_\mu^4} \ln \frac{m_e^2}{m_\mu^2} \\ &= 1 - 1.87 \times 10^{-4}. \end{aligned} \quad (5.99)$$

This result does not include the radiative corrections to muon-decay. The calculation of these corrections leads to additional correction  $f^{\text{rad}}$  and the decay rate is given by:

$$\Gamma = \Gamma_0(m_e = 0)f^{\text{rad}}, \quad (5.100)$$

and  $f^{\text{rad}}$  is given as:

$$f^{\text{rad}} = 1 - \frac{\alpha}{2\pi} \left( \pi^2 - \frac{25}{4} \right) \simeq 0.9958 \simeq 1 - 4.3 \times 10^{-3}. \quad (5.101)$$

Comparing the theoretical value of the decay rate,

$$\Gamma = \frac{G_\mu^2 m_\mu^5}{192\pi^3} f_e(m_e) f^{\text{rad}} \Rightarrow \tau = \frac{1}{\Gamma} = \frac{192\pi^3}{G_\mu^2 m_\mu^5 f_e f^{\text{rad}}} \quad (5.102)$$

with the experimental value of  $\tau = (2.19703 \pm 0.00004)\mu\text{s}$  and  $m_\mu = (105.658387 \pm 0.000034)\text{ MeV}$ , we obtain  $G_\mu = (1.166367 \pm 0.000004) \times 10^{-5} \text{ GeV}^{-2}$  which is very close to the value of  $G_F = (1.136 \pm 0.003) \times 10^{-5} \text{ GeV}^{-2}$  obtained from nuclear  $\beta$ -decay.

### (ii) The energy spectrum of the electron

After integrating over the angle  $(\theta, \phi)$ , we obtain for the energy distribution of the electron,

$$\frac{d\Gamma}{d\epsilon} = \frac{G_\mu^2 m_\mu^5}{192\pi^3} 2\epsilon^2 [3 - 2\epsilon], \quad (5.103)$$

where  $\epsilon = \frac{2E_e}{m_\mu}$ . The experimental results are in a very good agreement with the  $V - A$  theory of weak interactions. For an example, see the discussion in Ref.[238, 239].

### (iii) Electron helicity and parity violation

We see from Eq. (5.95) that the decay rate  $d\Gamma$  is nonzero only for  $\hat{n} \cdot \hat{s} = -1$  in the limit  $m_e \rightarrow 0$ , implying that the electron coming out of the muon-decay is left-handed. This result

is independent of energy, that is, the coefficient of  $\hat{n} \cdot \hat{s}$  is unity. It is also independent of energy in the limit of vanishing  $m_e$ . Thus, parity is maximally violated in muon-decay. This can be diagrammatically understood in a simple way considering the case of maximum energy, that is,  $\epsilon \simeq 1$  corresponding to the case when  $\bar{\nu}_e$  and  $\nu_\mu$  are emitted in the same direction (see Figure 5.9). Since  $\bar{\nu}_e$  and  $\nu_\mu$  have opposite helicities and move in the same direction, the total spin projection carried by the  $(\bar{\nu}_e, \nu_\mu)$  pair is zero. The spin carried by the electron is in the same direction as the muon. Since the direction of the emission of the electron is in the  $-Z$ -direction, its helicity is  $-1$  if the muon's spin is quantized in the  $+Z$ -direction. Therefore, the electrons emitted in the muon-decay are left-handed as in the case of  $\beta$ -decay.

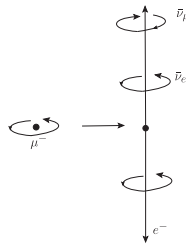


**Figure 5.9** A schematic representation of muon decay in case of maximum electron energy ( $\epsilon = 1$ ). Neutrinos have equal momenta and opposite spins. Hence, electron must be emitted in the opposite direction and has the spin in the same direction as that of the muon.

#### (iv) Electron asymmetry in the decay of polarized muons

We can write the angular distribution of the electrons from the decay of polarized muons as:

$$\frac{d\Gamma}{dE_e d\cos\theta} = K[A(E_e) + B(E_e)\cos\theta]\Theta(E_e^{\max} - E_e), \quad (5.104)$$

where (keeping  $m_e \neq 0$ )

$$K = \frac{G^2 m_\mu |\vec{p}_e| E_e}{12\pi^3}, A = 3E_e^{\max} - 2E_e - 2\frac{m_e^2}{E_e}, B = \frac{|\vec{p}_e|}{E_e} \left( E_e^{\max} - 2E_e + \frac{2m_e^2}{m_\mu} \right)$$

and  $E_e^{\max}$  is the maximum energy of the electron.

Under the parity transformation  $\theta \rightarrow \pi - \theta$ , where  $\theta$  is the angle between the muon's spin and the electron's momentum (as shown in Figure 5.10), that is, under this transformation,

$$\begin{aligned} \sin\theta &\xrightarrow{\theta \rightarrow \pi - \theta} +\sin\theta, \cos\theta \xrightarrow{\theta \rightarrow \pi - \theta} -\cos\theta, \\ \frac{d\Gamma(\pi - \theta)}{dE_e d\cos\theta} &\rightarrow K[A(E_e) - B(E_e)\cos\theta]. \end{aligned}$$

**Figure 5.10** Parity violation in the angular distribution.

Therefore,  $d\Gamma(\theta)$  and  $d\Gamma(\pi - \theta)$  are not the same, implying parity violation. The asymmetry parameter  $B$  is a measure of the parity violation.

After integrating over the electron's energy, the angular distribution  $d\Gamma/d\cos\theta$  is given by:

$$\frac{d\Gamma}{d\cos\theta} \sim K[1 - P\cos\theta], \quad (5.105)$$

that is, the electrons are emitted dominantly in the direction opposite to the spin of the muon, that is,  $\theta = \pi$ . Note that the asymmetry is  $\frac{P}{3}$ , where  $P$  is the magnitude of polarization of the initial muon. For a completely polarized muon along the  $\hat{z}$  direction ( $P = +1$ ), the asymmetry is  $A = \frac{1}{3}$ , which is to be compared with the experimental value of  $A = +0.325 \pm 0.005$  for  $e^+$  in the case of  $\mu^+$ -decay.

### 5.4.2 General structure of weak interaction in muon-decay and Michel parameters

The  $V - A$  structure of weak interactions was derived from the study of nuclear  $\beta$ -decays involving nucleons which were treated non-relativistically. Nevertheless, the process of muon-decay is also described very successfully using the  $V - A$  theory. Attempts were made to arrive at a theory of muon-decay using a fully relativistic treatment of the most general structure of the weak interaction Hamiltonian. We therefore consider once again the general structure of  $H_I^{\text{Weak}}(x)$  as:

$$\mathcal{H}_I^{\text{Weak}}(x) = \frac{G_\mu}{\sqrt{2}} \sum_i [\bar{u}_{\nu_\mu}(x) O_i u_\mu(x)] [\bar{u}_e(x) O^i (A_i - A'_i \gamma_5) u_{\nu_e}(x)], \quad (5.106)$$

where  $O_i = S, V, T, A, P$  operators are defined in terms of the Dirac gamma matrices in Eq. (5.106) and coefficients  $A_i$  and  $A'_i$  are the strength of various terms. The properties of the Dirac gamma matrices and the permutation symmetry between  $\mu^-, e^-, \bar{\nu}_e, \nu_\mu$  allows us to use the Fierz transformation [258] and write  $H_I^{\text{Weak}}$  in Eq. (5.106) as:

$$\mathcal{H}_I^{\text{Weak}}(x) = \frac{G_\mu}{\sqrt{2}} \sum_i [\bar{u}_e(x) O_i u_\mu(x)] [\bar{u}_{\nu_\mu}(x) O^i (C_i - C'_i \gamma_5) u_{\nu_e}(x)], \quad (5.107)$$

where the coefficients  $C_i$  and  $C'_i$  in Eq. (5.107) are given in terms of the coefficients  $A_i$  and  $A'_i$  used in Eq. (5.106) as:

$$C_i = \sum_j \Lambda_{ij} A_j, \quad C'_i = \sum_j \Lambda_{ij} A'_j \quad (5.108)$$

with [259]

$$\Lambda_{ij} = \frac{1}{4} \begin{pmatrix} 1 & 4 & 6 & 4 & 1 \\ 1 & -2 & 0 & 2 & -1 \\ 1 & 0 & -2 & 0 & 1 \\ 1 & 2 & 0 & -2 & -1 \\ 1 & -4 & 6 & -4 & 1 \end{pmatrix}.$$

One can check that the  $V - A$  structure remains invariant (from an overall sign) under the aforementioned permutation, that is,

$$\begin{aligned} C_V &= \frac{1}{4}(A_S - 2A_V + 2A_A - A_P), \\ C_A &= \frac{1}{4}(A_S + 2A_V - 2A_A - A_P), \\ C_V - C_A &= \frac{1}{4}(-4A_V + 4A_A) = -(A_V - A_A). \end{aligned} \quad (5.109)$$

Therefore, let us start with the most general Lorentz invariant, four Fermi point interaction matrix element for a muon-decay  $\mu^-(p_\mu) \rightarrow e^-(p_e) + \bar{\nu}_e(k_{\nu_e}) + \nu_\mu(k_{\nu_\mu})$  using Eq. (5.107)

$$\mathcal{M} = \frac{G}{\sqrt{2}} \sum_{i=S,V,A,T,P} \left[ \bar{u}_e(\vec{p}_e, s_e) \Gamma^i u_\mu(\vec{p}_\mu, s_\mu) \right] \left[ \bar{u}_{\nu_\mu}(\vec{k}_{\nu_\mu}, s_{\nu_\mu}) \Gamma_i (C_i - C'_i \gamma_5) u_{\nu_e}(\vec{k}_{\nu_e}, s_{\nu_e}) \right], \quad (5.110)$$

**Table 5.6** Michel parameters in  $V - A$  theory and their values determined in the experiments.

Michel parameter	$V - A$ values	Exp. values [117]
$\rho$	$\frac{3}{4}$	$0.74979 \pm 0.00017$
$\eta$	0	$0.057 \pm 0.034$
$\xi$	+1	$1.009^{+0.0016}_{-0.0007}$
$\delta$	$\frac{3}{4}$	$0.75047 \pm 0.0034$
$h$	+1	$1.00 \pm 0.04$

where  $\Gamma^i$  stand for the five bilinear covariants, viz., scalar (S), vector (V), axial vector (A), tensor (T), and pseudoscalar (P) terms having 1,4,4,6, and 1 components, respectively. To calculate decay rate,  $|\mathcal{M}|^2$  is required;  $|\mathcal{M}|^2$  should be proportional to the product of leptonic tensor ( $L_{e\mu}^{\alpha\beta}$ ) and the neutrino tensor ( $L_{\alpha\beta}^{\nu_\mu\nu_e}$ ), that is,

$$|\mathcal{M}|^2 = L_{e\mu}^{\alpha\beta} L_{\alpha\beta}^{\nu_\mu\nu_e}, \text{ where} \quad (5.111)$$

$$\begin{aligned} L_{\alpha\beta}^{\nu_\mu\nu_e} &= \sum_{i,j} \sum_{s_{\nu_\mu} s_{\nu_e}} \left[ \bar{u}_{\nu_\mu}(\vec{k}_{\nu_\mu}, s_{\nu_\mu}) \Gamma_\alpha^i (C_i - C'_i \gamma_5) u_{\nu_e}(\vec{k}_{\nu_e}, s_{\nu_e}) \right] \left[ \bar{u}_{\nu_e}(\vec{k}_{\nu_e}, s_{\nu_e}) (C_j^* + C_j'^* \gamma_5) \right. \\ &\quad \left. \Gamma_\beta^j u_{\nu_\mu}(\vec{k}_{\nu_\mu}, s_{\nu_\mu}) \right] \\ &= \sum_{i,j} \text{Tr} \left[ (A_{ij} \pm B_{ij} \gamma_5) \Gamma_\alpha^i \not{k}_{\nu_e} \Gamma_\beta^j \not{k}_{\nu_\mu} \right], \end{aligned} \quad (5.112)$$

$$A_{ij} = C_i C_j^* + C_i' C_j'^*, \quad B_{ij} = C_i C_j'^* + C_i' C_j^*$$

‘+’ sign is for S, P, and T terms and ‘−’ sign is for V and A terms.

$$\begin{aligned} L_{e\mu}^{\alpha\beta} &= \sum_{i,j} \sum_{s_e} [\bar{u}_e(\vec{p}_e, s_e) \Gamma_i^\alpha u_\mu(\vec{p}_\mu, s_\mu)] [\bar{u}_\mu(\vec{p}_\mu, s_\mu) \Gamma_j^\beta u_e(\vec{p}_e, s_e)] \\ &= \sum_{i,j} \text{Tr} \left[ \Gamma_i^\alpha (\not{p}_\mu + m_\mu) \frac{1 + \gamma_5 \not{p}_\mu}{2} \Gamma_j^\beta \not{p}_e \right]. \end{aligned}$$

Assuming that the muons are at rest and neglecting radiative corrections, the charged lepton energy spectrum is given by [259]:

$$\begin{aligned} \frac{d\Gamma(\mu)}{d\Omega dx} &= \frac{G_\mu^2 m_\mu^5}{192\pi^4} x^2 \left( \frac{1}{1 + 4\eta \frac{m_e}{m_\mu}} \left[ 4(x-1) + \frac{2}{3}\rho(4x-3) + 6\frac{m_e}{m_\mu} \frac{1-x}{x} \eta \right] \right. \\ &\quad \left. - \zeta \cos \theta_{\hat{s}, \hat{p}_e} \left[ (1-x) + \frac{2}{3}\delta(4x-3) \right] \right), \end{aligned} \quad (5.113)$$

$$x = \frac{E_e}{E_{\max}}, \quad E_{\max} = \frac{m_\mu}{2} \left( 1 + \frac{m_e^2}{m_\mu^2} \right), \quad x_0 = \frac{m_e}{E_{\max}}, \quad (5.114)$$

where  $\theta_{\hat{s}, \hat{p}_e}$  is the angle between the muon spin and the electron momentum.  $\rho$ ,  $\eta$ ,  $\zeta$ , and  $\delta$  of the aforementioned expression are known as Michel parameters [218] and are given in terms of the strengths of the various couplings  $C_i(C'_i)$  ( $i = S, V, T, A, P$ ) as [259]:

$$\begin{aligned} \rho &= \frac{1}{16} (3a_V + 6a_T + 3a_A), \quad \zeta = -\frac{1}{16} (4b' + 3a' - 14c'), \\ \eta &= \frac{1}{16} (a_S - 2a_V + 2a_A - a_P), \quad \delta = -\frac{1}{16\zeta} (3b' - 6c'), \end{aligned}$$

where  $a_i = |C_i|^2 + |C'_i|^2$ ,  $i = S, V, A, T, P$ .

$$\begin{aligned} a' &= 2\text{Re} (C_S C_P'^* + C'_S C_P^*), \quad b' = 2\text{Re} (C_V C_A'^* + C'_V C_A^*), \\ c' &= 2\text{Re} (C_T C_T'^*). \end{aligned}$$

The constants  $a_i$ s are constrained as  $a_S + 4a_V + 4a_A + 6a_T + a_P = 16$ , corresponding to the 16 components of the bilinear spinors. In case of a  $V - A$  interaction,  $C_S = C_P = C_T = C'_S = C'_P = C'_T = 0$  and  $C_V = C'_V = -C_A = -C'_A = 1$ . On the other hand, for SPT interaction,  $C_V = C'_V = C_A = C'_A = 0$ .

For the  $V - A$  interaction, Table 5.6 shows the predicted values of the Michel parameters  $\rho$ ,  $\eta$ ,  $\zeta$ , and  $\delta$  along with the experimental values, where a good agreement between the theoretical values predicted by the  $V - A$  theory and the experimental values can be seen.

### 5.4.3 Radiative corrections to $\mu$ -decays

Muons are charged particles which decay by emitting charged electrons and  $\bar{\nu}_e$  and  $\nu_\mu$ . Therefore, muon-decay is subject to the radiative corrections in which a photon is emitted by the charged particles and is reabsorbed. Diagrammatically, they are shown in Figure 5.11(a),(b)



and (c); which contribute to the radiative corrections in the lowest order in perturbation theory. The figures correspond to the loop diagrams discussed in Chapter 4. The radiative corrections are categorized as the (i) vertex correction (Figure 5.11(a)) and the (ii) self-energy diagram (Figure 5.11(b) and 5.11(c)). The diagrams corresponding to the charged particle Bremsstrahlung in which a photon is emitted from a charged particle as shown in Figures 5.11(d) and 5.11(e) are also considered in addition to the loop diagrams because the very low energy real photons, which are emitted below the threshold of experimental detection, are indistinguishable from those which are emitted and re-absorbed. The early calculations of

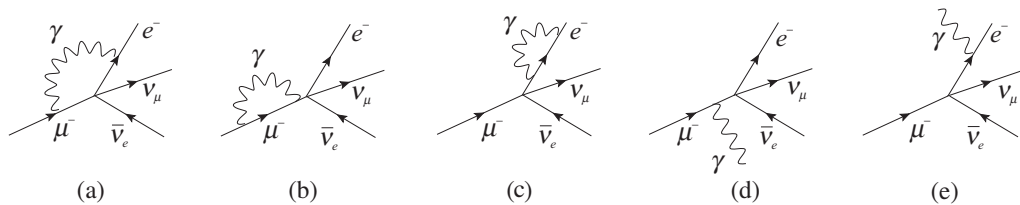


**Figure 5.11** The higher order corrections to the muon-decay: (a) Vertex correction, (b, c) Self energy correction and (d, e) Bremsstrahlung contributions.

these diagrams using QED have been done by Behrends et al. [260], Knoshita and Sirlin [261], Berman and Sirlin [262], and Berman [263]. For a detailed review, please see Ref.[264]. The Bremsstrahlung diagrams, Figure 5.11(d) and 5.11(e), help to remove the infrared divergences due to the other diagrams. Ultraviolet divergences are removed by using the renormalization procedure to regularize the divergent integrals in an appropriate gauge using Ward's identities. In the case of  $V - A$  theory, one finds the following correction to the momentum (energy) distribution [239]:

$$\frac{d\Gamma^{\text{corrected}}}{dx} = \frac{d\Gamma^{\text{uncorrected}}}{dx} (1 + f(x)); \quad x = \frac{|\vec{p}_e|}{|\vec{p}_e^{\text{max}}|}, \quad (5.115)$$

where

$$\begin{aligned} f(x) &= \frac{1}{3-2x} \frac{\alpha}{2\pi} \left[ (6-4x)R(x) + (6-6x)\ln(x) + \frac{1-x}{3x^2} \right. \\ &\quad \left. \left\{ (5+17x-34x^2)(\omega + \ln(x))(-22x+34x^2) \right\} \right] \\ R(x) &= 2 \sum_{n=1}^{\infty} \frac{x^n}{n^2} - \frac{\pi^2}{3} - 2 + \omega \left( \frac{3}{2} + 2 \ln \frac{1-x}{x} \right) \\ &\quad - \ln(x)(2 \ln(x) - 1) + (3 \ln(x) - 1) - \frac{1}{x} \ln(1-x). \\ \omega &= \ln \frac{m_\mu}{m_e}, \end{aligned}$$

leading to the following modification in the decay rate (in the limit  $m_e \rightarrow 0$ ), resulting in:

$$\Gamma_{\text{corrected}} = \frac{G_\mu^2 m_\mu^5}{192\pi^3} \left[ 1 - \frac{\alpha}{2\pi} \left( \pi^2 - \frac{25}{4} \right) \right] \approx 0.9958, \quad (5.116)$$

where  $\frac{G_\mu^2 m_\mu^5}{192\pi^3}$  is the uncorrected value of the decay rate  $\Gamma$ ; numerically, the corrections are very small  $\approx 0.4\%$ . Using Eq. (5.116), one obtains a precise value of  $G_\mu$  by taking the measured lifetime  $\tau = \frac{1}{\Gamma}$  and mass of the muons as the inputs. The calculation of the radiative corrections shown in Figure 5.11 and the higher order diagrams are beyond the scope of this book; readers are referred to [264].

## 5.5 Inverse Muon-decay and $\nu_\mu$ Scattering

Muon-decay is represented by the reaction

$$\mu^- \rightarrow e^- + \bar{\nu}_e + \nu_\mu$$

and the inverse muon-decay process would be a scattering process like:

$$\nu_e + \mu^- \rightarrow e^- + \nu_\mu \quad \text{or} \quad \nu_\mu + e^- \rightarrow \mu^- + \nu_e$$

depending upon the incident beam and the target. Since preparing a muon target is difficult due to the muon being an unstable particle, the reaction  $\nu_\mu + e^- \rightarrow \mu^- + \nu_e$  with  $\nu_\mu$  beams and an electron target is more amenable to experiments. Such experiments have been done at CERN SPS [265], Fermilab Tevatron [266], and CHARM II at CERN [267]. In this section, we show the calculation of the cross section for this process in  $V - A$  theory, in the first order of perturbation theory. The Feynman diagram for these processes is shown in Figure 5.12. The matrix element  $\mathcal{M}$  corresponding to the Feynman diagram shown in Figure 5.12 is

$$\mathcal{M} = \frac{G_\mu}{\sqrt{2}} [\bar{u}_{\nu_e}(k', s'_{\nu_e}) \gamma_\mu (1 - \gamma_5) u_e(p, s_e)] [\bar{u}_\mu(p', s'_e) \gamma^\mu (1 - \gamma_5) u_{\nu_\mu}(k, s_{\nu_\mu})], \quad (5.117)$$

where  $(k, s_{\nu_\mu})$ ,  $(k', s'_{\nu_e})$  are the momenta and spin of initial and final neutrinos,  $\nu_\mu$  and  $\nu_e$  and  $(p, s_e)$ ,  $(p', s'_e)$  are the momenta and spin of the initial and final charged leptons  $e$  and  $\mu$ .

Following standard methods for calculating the differential cross section, we write:

$$\begin{aligned} d\sigma &= \frac{(2\pi)^4 \delta^4(p + k - p' - k')}{4((k.p)^2 - m_\nu^2 m_e^2)^{\frac{1}{2}}} \Pi \frac{d\vec{p}'}{(2\pi)^3 p'_0} \frac{d\vec{k}'}{(2\pi)^3 k'_0} \sum_{\text{spins}} |\mathcal{M}|^2 \\ &= \frac{1}{(2\pi)^2} \frac{\delta^4(p + k - p' - k')}{4k.p} \frac{d\vec{p}'}{p'_0} \frac{d\vec{k}'}{k'_0} \sum \sum |\mathcal{M}|^2. \end{aligned} \quad (5.118)$$

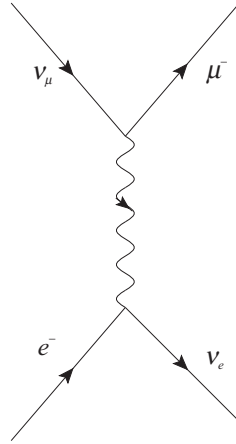


**Figure 5.12** Inverse muon decay:  $\nu_\mu + e^- \rightarrow \mu^- + \nu_e$ .

The spin sums  $\sum_i \sum_f |\mathcal{M}|^2$  is calculated in a way similar to the calculations done in muon- decay with the result:

$$\sum_i \sum_f |\mathcal{M}|^2 = 64 G_\mu^2 (k \cdot p)(k' \cdot p').$$

Since  $k' \cdot p' = \frac{1}{2}(s - m_\mu^2)$ , where  $s = 4E_\nu^2$  is the CM (center of mass) energy of the neutrino. We get:

$$\frac{d\sigma}{d\Omega} = \frac{G_\mu^2}{2\pi^2} (s - m_\mu^2) \int \frac{d\vec{p}'}{p'_0} k'_0 dk'_0 \delta^4(p + k - p' - k').$$

Performing the momentum integration over  $p'$ , we obtain:

$$\begin{aligned} \frac{d\sigma}{d\Omega} &= \frac{G_\mu^2}{2\pi^2} (s - m_\mu^2) \frac{s - m_\mu^2}{2s} \\ &= \frac{G_\mu^2}{4\pi^2} s \left(1 - \frac{m_\mu^2}{s}\right)^2, \end{aligned} \quad (5.119)$$

where we have used

$$\int \int \frac{d\vec{p}'}{p'_0} k'_0 dk'_0 \delta^4(p + k - p' - k') = \frac{s - m_\mu^2}{2s}, \quad (5.120)$$

which, in the high energy limit  $s \gg m_\mu^2$  gives:

$$\frac{d\sigma}{d\Omega} = \frac{G_\mu^2 s}{4\pi^2} \quad \text{and} \quad \sigma = \frac{G_\mu^2 s}{\pi} = \frac{4G_\mu^2}{\pi} E_\nu^2, \quad (5.121)$$

where  $E_\nu$  is the energy of the incident neutrino in CM. The standard model prediction for the inverse muon-decay is  $\sigma = 17.23 \times E_\nu(\text{GeV}) \times 10^{-42} \text{cm}^2/\text{GeV}$ . This is in good agreement with the experimentally observed values of  $(16.93 \pm 0.85 \pm 0.52) \times E_\nu(\text{GeV}) \times 10^{-42} \text{cm}^2/\text{GeV}$  by CCFR collaboration at the Fermilab [266] and  $(16.51 \pm 0.93) \times E_\nu(\text{GeV}) \times 10^{-42} \text{cm}^2/\text{GeV}$  by Bergsma et al. [267] at CERN using the wide band beam.

The calculation done in the lowest order perturbation theory shows that the cross section increases with energy as  $E_\nu^2$ . The differential cross section  $\frac{d\sigma}{d\Omega}$  given in Eq. (5.119) is isotropic showing that it is an s-wave scattering. It is well-known that the s-wave scattering amplitude and the scattering cross section is bounded by the principle of unitarity and cannot exceed the unitarity limit as energy increases. At some energy  $E_\nu$ , the cross section calculated earlier will violate the principle of unitarity, which predicts that  $\frac{d\sigma}{d\Omega} \leq \frac{1}{4E_\nu^2}$ . The fact that the higher order calculations in perturbation expansion using Fermi theory and also the  $V - A$  theory do not solve this problem of the violation of unitarity, was realized long back by Fierz [258] and Heisenberg [268]. This is one of the limitations of  $V - A$  theory and will be discussed in some detail in Section 5.7.

## 5.6 Muon Capture and $\mu - e$ Universality

Historically, the leptonic decay of muon has been the most studied process following its discovery. The evidence that muons also interact weakly with nucleons was soon reported by Conversi et al. [269] by observing the process of the weak muon capture in heavy nuclei through the process  $\mu^- + p \rightarrow n + \nu_\mu$ . With improved experimental techniques, the process of  $\mu$  capture was also observed later in light nuclei like  $^3\text{He}$  and  $^{12}\text{C}$ , though the observation of muon capture in protons could only be made in 1962 [270]. In this process, the muon is absorbed by the proton in nuclei before decaying into electrons and only one neutrino is produced. The process competes with the decay process  $\mu^- \rightarrow e^- + \bar{\nu}_e + \nu_\mu$  in the nucleus and dominates for  $Z \geq 6$ . Since its first observation, the process of nuclear muon capture has been studied in numerous experiments involving complex nuclei. Theoretically, it was discussed in the early days by Pontecorvo [112], Fermi, Teller and Weisskopf [271]. The weak process of ordinary K-capture of electrons from nuclei, that is,  $e^- + p \rightarrow n + \nu_e$  was already predicted by Yukawa and Sakata [272] and observed by Alvarez [273]. Later, a comparative study of muon capture in nuclei, electron capture in nuclei, muon decay, and nuclear  $\beta$ -decay was made by Tiomno and Wheeler [115], Lee, Rosenbluth and Yang [274] and Puppi [113] and Klein [114]. It was shown that the strength of the coupling in  $\mu$  decay,  $e^-$  capture,  $\mu^-$  capture, and  $\beta$ -decay in nuclei are close to each other as far as Fermi interactions are concerned. This suggested the principle of universal Fermi interaction (UFI) for the first time and implies that the strength of the Fermi interaction, that is, the vector current interaction is the same for the electrons and muons in their interaction with the nucleons and nuclei and  $G_F \approx G_\mu$ . This is known as  $\mu - e$  universality.

In the case of  $\mu^-$  capture at rest, the energy transferred to the nuclear system is of the order of  $m_\mu$  (100 MeV) and momentum transfer  $q^2 (\approx m_\mu^2)$  is large as compared to the energies involved in a nuclear  $\beta$ -decay. Therefore, the structure of the matrix elements of the  $V - A$

currents, taken between the nucleon states, involves more terms in addition to the  $C_V$  and  $C_A$  terms which depend upon momentum. The additional term in the matrix element of the vector current term is proportional to  $\bar{u}_p \sigma_{\mu\nu} q^\nu u_n(p)$  and is known as the weak magnetism term; and in the axial term is proportional to  $\bar{u}_p(p') q^\mu \gamma_5 u_n(p)$  and is known as the pseudoscalar term. The process of muon capture in nuclei plays a very important role in determining the strength of coupling of these terms, specially in the case of the pseudoscalar term. This is because the pseudoscalar term can be shown to be proportional to the mass of the lepton and is therefore negligible in all weak processes involving electrons. The reactions with muons in the initial or final state are the only reactions where the pseudoscalar term is determined specially at very low energies. In the region of low energy weak interactions involving nuclei, the muon capture plays a major role, in determining the pseudoscalar coupling as emphasized in the work of Goldberger-Trieman [275], Leite Lopes [276], and Wolfenstein [277].

## 5.7 Limitations of the Phenomenological Theory

### 5.7.1 High energy behavior of $\nu_l - l^-$ scattering and unitarity

We consider the reactions  $\nu_l(k) + l^-(p) \rightarrow l^-(k') + \nu_l(p')$ , ( $l = e, \mu$ ) with  $k(k')$  and  $p(p')$  being the momenta of the initial (final) neutrino and lepton respectively; they are calculated in the theory using the  $(J^l)_\mu^\dagger (J^l)^\mu$  piece of interaction Hamiltonian  $H_{\text{int}}(x)$  given in Eq. (5.106).

We obtain the cross section  $\frac{d\sigma}{d\Omega}$  and the total scattering cross section  $\sigma$ , in the CM frame, as:

$$\frac{d\sigma}{d\Omega} = \frac{G_F^2 s}{4\pi^2} \left(1 - \frac{m_l^2}{s}\right)^2, \quad (5.122)$$

$$\sigma = \frac{G_F^2 s}{\pi} \left(1 - \frac{m_l^2}{s}\right)^2, \quad (5.123)$$

where  $s$  is the center of mass (CM) energy of the  $\nu_l$  and  $l^-$ , that is,  $s = (p + k)^2$ . For the present purpose of taking high energy limit, we can neglect the second term as  $m_l^2 \ll s$  and obtain:

$$\sigma = \frac{G_F^2}{\pi} s. \quad (5.124)$$

We note that

- i) The angular distribution is isotropic.
- ii) The total cross section increases with energy.

In general, the two-particle scattering amplitude  $f(\theta)$  can be expanded in terms of the partial wave amplitudes as:

$$f(\theta) = \frac{1}{|\vec{p}_{CM}|} \sum_{J=0}^{\infty} \left(J + \frac{1}{2}\right) \mathcal{M}_J P_J(\cos \theta), \quad (5.125)$$

where  $\vec{p}_{CM}$  is the momentum of the incident particle in the CM frame and  $\mathcal{M}_J$  is the amplitude in the  $J$ th partial wave. In the CM frame,  $\vec{k} + \vec{p} = 0$  and  $s = (k + p)^2 = (k_0 + p_0)_{CM}^2$ ,

$$\begin{aligned} s &= \left( \sqrt{m_e^2 + |\vec{k}|^2} + \sqrt{m_\nu^2 + |\vec{p}|^2} \right)^2 = m_e^2 + |\vec{k}|^2 + m_\nu^2 + |\vec{p}|^2 \\ &\quad + 2\sqrt{m_e^2 + |\vec{k}|^2} \sqrt{m_\nu^2 + |\vec{p}|^2} \\ &\simeq 4|\vec{p}_{CM}|^2, \text{ in the limit } m_e, m_\nu \rightarrow 0. \end{aligned} \quad (5.126)$$

We find the differential scattering cross section in the CM frame as:

$$\begin{aligned} \frac{d\sigma}{d\Omega} &= |f(\theta)|^2 = \frac{1}{4|\vec{p}_{CM}|^2} \left| \sum_{J=0}^{\infty} (2J+1) \mathcal{M}_J P_J(\cos\theta) \right|^2 \\ \text{leading to } \frac{d\sigma}{d\Omega} &= \frac{1}{4|\vec{p}_{CM}|^2} |\mathcal{M}_0|^2 \end{aligned}$$

as only  $J = 0$  contributes, because the  $\nu_e e^-$  interaction is local in  $V - A$  theory. This leads to:

$$\sigma = \frac{\pi}{|\vec{p}_{CM}|^2} |\mathcal{M}_0|^2 = \frac{4\pi}{s} |\mathcal{M}_0|^2. \quad (5.127)$$

The unitarity of the  $S$  matrix, that is,  $S^\dagger S = 1$  implies that the scattering amplitude  $\mathcal{M}_J$  in the  $J$ th partial wave can be written as:

$$\mathcal{M}_J = e^{i\delta_J} \sin \delta_J,$$

where  $\delta_J$  is the phase shift. This implies an upper bound for  $\mathcal{M}_J$ , that is,  $|\mathcal{M}_J| \leq 1$  for each  $J$ .

We, therefore, find a unitarity upper limit for  $\sigma(\nu_l e^- \rightarrow l \nu_e) = \frac{4\pi}{s}$ . Since the phenomenological theory predicts that the cross section increases with  $s$ , that is,  $\frac{G^2 s}{\pi}$ , if  $\frac{G^2 s}{\pi} \geq \frac{4\pi}{s}$ , then the unitarity limit is violated. This implies that for the CM energy of  $s \geq \frac{2\pi}{G}$ , the unitarity limit is violated. This corresponds to the lab energy of

$$E_v^{lab} = \frac{s}{2m_e} = \frac{\pi}{m_e G} \approx 6 \times 10^8 \text{ GeV}.$$

This is too high an energy to be tested in the laboratory but in principle, the theory violates unitarity at very high energies of  $E \approx 10^8$  GeV when the cross sections are calculated in the lowest order of perturbation theory.

### 5.7.2 Divergence and renormalization

The problem of the violation of the unitarity described in the previous section arises in the first order calculations of the neutrino–electron scattering cross section using perturbation theory. The higher order contributions to  $\nu_l e^-$  scattering should also be considered. The contribution in the higher order of perturbation theory comes due to the diagrams shown in Figure 5.13. The

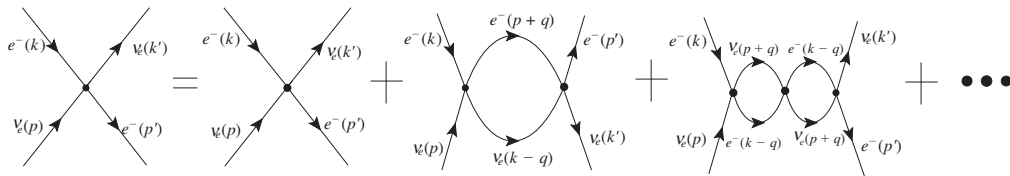


**Figure 5.13** First order, second order, and higher order diagrams in  $V - A$  theory for  $\nu_e - e^-$  scattering.

matrix element  $\mathcal{M}(2)$  for the second order diagram is

$$\begin{aligned} \mathcal{M}(2) &\propto G_F^2 \int \frac{d^4 q}{(2\pi)^4} \left[ \bar{u}_e(p', s') \gamma_\mu (1 - \gamma_5) \frac{1}{\not{p} + \not{q} - m_e} \gamma_\nu (1 - \gamma_5) u_e(p, s) \right] \\ &\times \left[ \bar{u}_{\nu_e}(k', t') \gamma^\mu (1 - \gamma_5) \frac{1}{\not{k} - \not{q}} \gamma^\nu (1 - \gamma_5) u_{\nu_e}(k, t) \right] + \dots \end{aligned} \quad (5.128)$$

The high energy behavior of this integral can be understood by counting the powers of the momentum  $\vec{q}$  in the numerator and the denominator of the integrand, which behave like

$$\mathcal{M}(2) \propto \int_0^\infty \frac{d^4 q}{q^2} \simeq \int_0^\infty \frac{q^3 dq}{q^2} \simeq \int_0^\infty q dq \quad (5.129)$$

and therefore diverges. The higher order diagrams give even more divergent integrals. This was realized quite early by Heisenberg [268] and Fierz [258]. Such divergences also occur in QED but they are absorbed to all orders, in terms of the renormalization of the charge, mass, and the vertex function. In this case, divergence of such integrals appear in all orders requiring a new renormalization constant each time. The Fermi theory and the phenomenological  $V - A$  theory is, therefore, not renormalizable. This is one of the major difficulties faced by the  $V - A$  theory.

In order to solve this problem, it was suggested quite early in the development of the phenomenological theory that if the charged current weak interactions are mediated by massive vector bosons like the electromagnetic interactions are mediated by vector  $A_\mu$  fields, then the additional  $q^2$  dependence of the massive vector boson propagator may help to solve the problem of divergence. However, the IVB theory did not succeed in removing the divergence.

### 5.7.3 Intermediate vector boson (IVB) theory

In this theory, the weak interaction of leptons/nucleons is mediated by the vector bosons  $W_\mu^\pm$  with the interaction Hamiltonian given by:

$$\mathcal{H} = g_W J_\mu^\dagger W^\mu + \text{h.c.}, \quad (5.130)$$

where  $g_W$  is the weak coupling strength.

The  $\nu_e - e^-$  scattering is then described in the lowest order by the Feynman diagram shown in Figure 5.14.

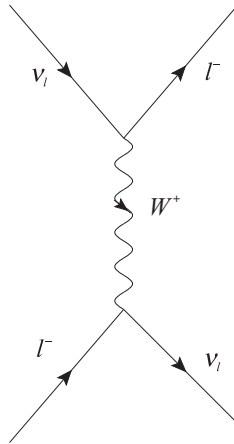


**Figure 5.14**  $\nu_l - l^-$  scattering mediated by  $W^+$  boson.

The matrix element  $\mathcal{M}$  is written as:

$$\mathcal{M} = g_W^2 \bar{u}_e \gamma_\mu (1 - \gamma_5) u_{\nu_e} D^{\mu\nu} \bar{u}_{\nu} \gamma_\nu (1 - \gamma_5) u_e, \quad (5.131)$$

$$\text{where } D^{\mu\nu} = -i \frac{\left( g^{\mu\nu} - \frac{q^\mu q^\nu}{M_W^2} \right)}{q^2 - M_W^2}$$

is the  $W^\pm$  propagator with  $M_W$  being the mass of  $W^\pm$  bosons. For small values of  $q^2$  implying  $q^2 \ll M_W^2$ , Eq. (5.131) reduces to the expression obtained using  $V - A$  theory provided

$$\frac{g_W^2}{M_W^2} \approx \frac{G_F}{\sqrt{2}}.$$

Carrying out the computation for the cross section in the CM frame using the expression of the amplitude from Eq. (5.131), we obtain:

$$\frac{d\sigma}{d\Omega} = \frac{1}{64\pi^2 s} |\mathcal{M}|^2 \quad (5.132)$$

$$\Rightarrow \frac{d\sigma}{d\Omega} = \frac{2g_W^4 |\vec{k}|^2}{\pi^2 (q^2 - M_W^2)^2}, \quad (5.133)$$

where  $|\vec{k}|$  is the momentum of the initial particle in the CM frame. This leads to:

$$\sigma = \frac{4G_F^2 |\vec{k}|^2}{\pi} \left( 1 + \frac{4|\vec{k}|^2}{M_W^2} \right)^{-1}, \quad (5.134)$$



in which  $k^2 \ll M_W^2$  limit gives the  $V - A$  result, that is,

$$\sigma = \frac{G_F^2}{\pi} s$$

and in the limit  $|\vec{k}| \rightarrow \infty$ ,

$$\sigma = \frac{G_F^2 M_W^2}{\pi} = \text{constant.}$$

thus preventing the violation of the unitarity limit. However, the partial wave unitarity in the S-wave is still violated. It can be shown that the partial wave amplitude in the S-wave,  $f_0$  corresponding to the transition amplitude calculated in the  $W$  exchange is given by [278]:

$$f_0 = \frac{G_F M_W^2}{\sqrt{2}\pi} \log \left( 1 + \frac{4|\vec{k}^2|}{M_W^2} \right)$$

which still violates the unitarity limit, that is,

$$f_0 > 1, \text{ for } k \approx \frac{M_W}{2} \exp \left( \frac{\pi}{\sqrt{2} G_F M_W^2} \right).$$

In the second order of the perturbation theory in the IVB theory, there would be two IVB propagators bringing additional  $q^2$  dependence proportional to  $(q^2)^2$  in the denominator, making the loop integral in the diagram behave as:

$$M^{(2)} \sim \int \frac{d^4 q}{q^2} \frac{1}{(q^2)^2} \approx \int \frac{dq}{q^3},$$

which is no longer divergent as  $q \rightarrow \infty$ . It should be noted that the term proportional to  $q^\mu q^\nu$  in the numerator of the  $W$  propagator does not contribute when contracted with the leptonic part in  $q^\mu l_\mu$  as  $q^\nu l_\nu \sim 0$  in the limit of  $m_e \rightarrow 0$ . Thus, the processes in which the IVB appear in virtual state are not divergent in the IVB theory.

However, the situation is quite different in the processes, where real IVB's are produced that is,  $\nu_\mu + \bar{\nu}_\mu \rightarrow W^+ + W^-$  as shown in Figure 5.15.

The matrix element  $\mathcal{M}$  for this process is written as:

$$\begin{aligned} \mathcal{M} \propto & g_W^2 \epsilon_\mu^{-*}(k_2, \lambda_2) \epsilon_\nu^{+*}(k_1, \lambda_1) \\ & \times \bar{v}(p_2) \gamma^\mu (1 - \gamma_5) \frac{1}{(\not{p}_1 + \not{p}_2) - m_l} \gamma^\nu (1 - \gamma_5) u(p_1), \end{aligned} \quad (5.135)$$

where  $\epsilon_\mu$  and  $\epsilon_\nu$  are the polarization vectors of the  $W^\mu$  bosons, that is,  $\epsilon_\mu^{-*}(k_2, \lambda_2)$  is associated with  $W^-$  and  $\epsilon_\nu^{+*}(k_1, \lambda_1)$  with  $W^+$ ;  $k_1$  and  $k_2$  are four momenta; and  $\lambda_1$  and  $\lambda_2$  are the polarization states of  $W^+$  and  $W^-$  respectively. In order to calculate  $\sum_{\text{spins}} |\mathcal{M}|^2$ , we have to

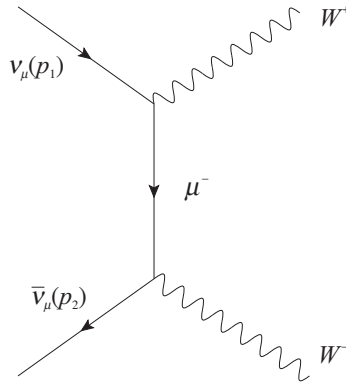


**Figure 5.15** Feynman diagram depicting  $\nu_\mu \bar{\nu}_\mu \rightarrow W^+ W^-$  via  $\mu^-$  exchange.

sum over the polarization states of  $W_\mu^+$  and  $W_\mu^-$  using:

$$\sum_{\lambda=0,\pm 1} \epsilon_\mu(k, \lambda) \epsilon_\nu^*(k, \lambda) = -g_{\mu\nu} + \frac{k_\mu k_\nu}{M_W^2}. \quad (5.136)$$

Since we are interested in the high energy behavior of the cross section, we consider the contribution of the  $\frac{k_\mu k_\nu}{M_W^2}$  term in Eq. (5.136). It can be shown that this momentum dependent term comes from the longitudinal component of the polarization vector  $\epsilon_\mu(k, \lambda)$  of the  $W$  bosons (Chapter 2). We, therefore, calculate the  $\sum_{\text{spin}} |\mathcal{M}_{00}|^2$  term corresponding to the production of the longitudinally polarized  $W$  bosons. The following result is obtained for  $\sum |\mathcal{M}_{00}|^2$ , using Eqs. (5.135) and (5.136) [278, 279]

$$\sum |\mathcal{M}_{00}|^2 \sim \frac{g_W^4}{M_W^4} (p_1 \cdot k_1) (p_2 \cdot k_2) \sim \frac{g_W^4}{M_W^4} E^4 (1 - \cos^2 \theta), \quad (5.137)$$

where  $E$  is the CM energy and  $\theta$  is the CM scattering angle. Using this equation, we find

$$\frac{d\sigma}{d\Omega}(\nu_\mu \bar{\nu}_\mu \rightarrow W^+ W^-) = G_F^2 \frac{E^2 \sin^2 \theta}{8\pi^2} \quad (5.138)$$

the energy dependence of the differential cross section similar to the result for the differential cross section for the process  $\nu e^- \rightarrow \nu e^-$ , leading to the violation of unitarity. Therefore, the IVB model has the same problems of bad high energy behavior of the cross section as the local  $V - A$  theory. This is the main reason for the lack of renormalization in the phenomenological theory, even in the presence of intermediate vector bosons.

### 5.7.4 Radiative corrections

Another difficulty of considerable importance was faced by the Fermi type theory as well as the IVB type theory, which relates to the bad high energy behavior in the calculation of radiative

correction to weak processes. One finds that in the leptonic sector, the radiative corrections to the  $\mu$ -decay are finite, but the corrections to  $\nu_e + e^- \rightarrow \nu_e + e^-$  diverge in the order  $\alpha^2$ . In the case of the semileptonic sector, like  $n \rightarrow p + e^- + \bar{\nu}_e$ , the corrections diverge in order  $\alpha$  even in the absence of strong interactions. The presence of form factors due to the structure of hadrons, which are expected to provide damping of the amplitude with increasing  $E$  and  $q^2$ , do not help to cure the divergences. The divergences appear both in the vector as well as in the axial vector contributions and do not cancel with each other. The problem essentially arises due to the bad high energy behavior of the transition amplitudes when calculated in the higher orders of perturbation because of the non-renormalizability of the theory. Numerous attempts were made to explain this difficulty without success [280]. The problem of radiative corrections could be solved only after the formulation of the unified theory of electroweak interactions, which came in the early 1970s.

## 5.8 $\tau$ Lepton and Its Weak Decays and $e - \mu - \tau$ Universality

### 5.8.1 $\tau$ lepton and its properties

The tau( $\tau$ ) lepton first discussed theoretically by Tsai [281] and Thacker and Sakurai [282] in 1971, was discovered in 1975 by Perl et al. [116] at the SPEAR storage ring in the SLAC-LBL laboratory and later by Burmester et al. [283] at DESY in 1977. For a detailed review, please see Ref. [284]. In a storage ring, the electron and positron beams circulate in opposite directions and are forced to collide in a region where detectors are placed for observing the final particles produced in the collision, like electrons, muons, and hadrons within a large solid angle. In the  $e^+e^-$  collision experiments, a number of anomalous events with electrons and muons like  $e^-\mu^+$  or  $e^+\mu^-$  pairs, accompanied by some neutral particles, that is in the reaction,  $e^- + e^+ \rightarrow e^- + \mu^+$  and at least two unobserved particles, were reported. Since the lepton number is conserved,  $e^\pm\mu^\mp$  cannot be produced through a direct interaction but only as decay products of some intermediate particles produced in the collision process of  $e^-$  and  $e^+$ , consistent with the conservation of both lepton numbers  $L_e$  and  $L_\mu$ .

These intermediate particles could be heavy hadrons or leptons. The threshold energy for the production of these  $e^\pm\mu^\mp$  events was in the region of 3.6 – 4.0 GeV. A characteristic feature of these  $e^\pm\mu^\mp$  events was that with increase in energy, the electrons and muons were collinearly emitted in opposite directions indicating that they are most likely the decay products of a particle–antiparticle pair produced in the collision.

The threshold energy of 3.6 – 4.0 GeV implies that these particles  $\tau^{-(+)}$  would have a mass  $m \geq 1.7$  GeV. This expectation is consistent with the earlier results from CERN [284] that there are no heavy leptons with mass  $m \leq 1.5$  GeV. These particles could be heavy leptons, undergoing three body decays like muons

$$\tau^{-(+)} \rightarrow e^-(e^+) + \nu_\tau(\bar{\nu}_\tau) + \bar{\nu}_e(\nu_e), \tau^-(\tau^+) \rightarrow \mu^-(\mu^+) + \nu_\tau(\bar{\nu}_\tau) + \bar{\nu}_\mu(\bar{\nu}_\mu). \quad (5.139)$$

The other possibilities are that the  $e^-\mu^+$  pairs come from the intermediate state where two photons are produced through the reaction  $e^+e^- \rightarrow 2\gamma \rightarrow e^+e^-, \mu^+\mu^-$  or through the sequential decays of heavy baryons or bosons produced in the  $e^-e^+$  collision. All these processes would yield an  $e^-\mu^+$  energy spectrum which carries the characteristic signatures of the parent intermediate particle produced in the  $e^-e^+$  collisions. A detailed analysis of the energy (momentum) distribution of  $e^-(e^+)$  and  $\mu^+(\mu^-)$  emitted in these processes ruled out the possibility of the intermediate particle being heavy bosons, photons, or heavy hadrons. The signature of the intermediate particles being heavy leptons was the most likely, and these particles were called  $\tau$  leptons.

The properties of  $\tau$  leptons like their mass, lifetime, spin, and their structure were determined by studying the observable  $R_{e\mu}(s)$  and  $R_{eh}(s)$  ( $\sqrt{s}$  is the CM energy) defined as

$$R_{e\mu} = \frac{\sigma(e^+e^- \rightarrow \tau^+\tau^- \rightarrow e\mu)}{\sigma(e^+e^- \rightarrow \mu^+\mu^-)}, \quad (5.140)$$

$$R_{eh} = \frac{\sigma(e^+e^- \rightarrow \tau^+\tau^- \rightarrow eh)}{\sigma(e^+e^- \rightarrow \mu^+\mu^-)}, \quad (5.141)$$

where  $h$  is hadron.

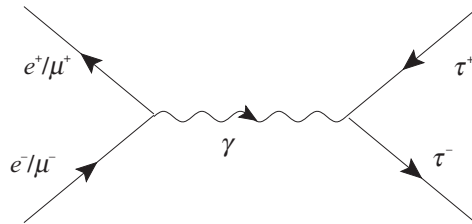


**Figure 5.16**  $e^-e^+(\mu^-\mu^+) \rightarrow \tau^-\tau^+$  process mediated by a photon exchange.

Using the standard procedure for calculating cross sections for  $e^-e^+$  collisions and assuming photon exchange corresponding to Figure 5.16, the cross section  $\sigma_{\tau\tau}$  for the process  $e^+e^- \rightarrow \tau^+\tau^-$  is given by:

$$\sigma_{\tau\tau} = \sigma_{\mu\mu} |F_\tau(s)|^2 F(\beta), \quad (5.142)$$

where

$$\sigma_{\mu\mu} = \frac{4\pi\alpha^2}{3s} \quad (5.143)$$

is the cross section for  $e^+e^- \rightarrow \mu^+\mu^-$ .  $F(\beta)$  is a function of the velocity  $\beta (= \frac{|\vec{p}|}{E})$  of  $\tau^+$  given by:

$$F(\beta) = \frac{1}{4}\beta^3 \quad \text{for spin } 0, \quad (5.144)$$

$$= \frac{1}{2}\beta(3 - \beta^2) \quad \text{for spin } \frac{1}{2}, \quad (5.145)$$

$$= \beta^3 \left[ \left( \frac{s}{4m_\tau^2} \right)^2 + 5 \frac{s}{4m_\tau^2} + \frac{3}{4} \right] \quad \text{for spin 1,} \quad (5.146)$$

and  $F_\tau(s)$  is the form factor at the  $\gamma\tau^+\tau^-$  vertex (Figure 5.16) and taken to be

$$F_\tau(s) = 1 \pm \frac{s}{\Lambda_\pm^2}, \quad (5.147)$$

where  $\Lambda$  is the cut-off parameter. In Figure 5.17, we show the behavior of  $R_{eh}$  and  $R_{e\mu}$  for

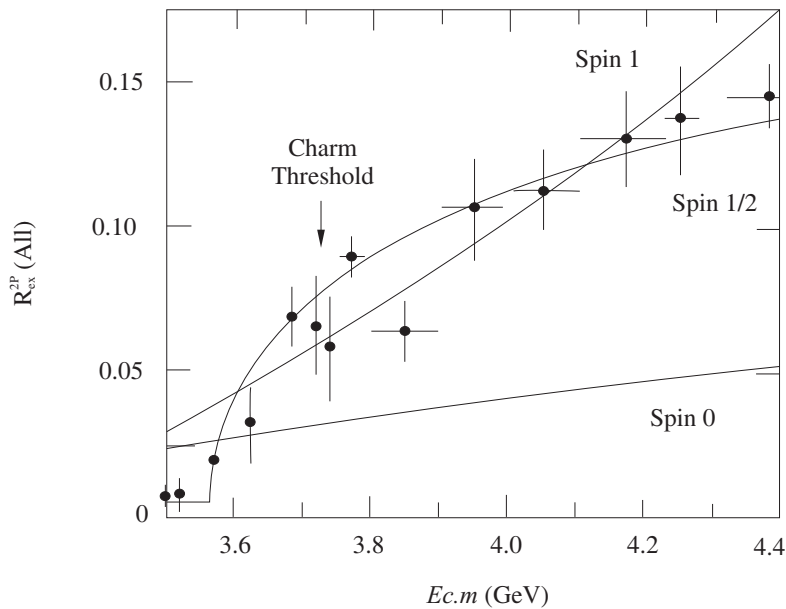


**Figure 5.17** The production cross section ratio  $R_{eX}^{2p} = \frac{\sigma(e^+e^- \rightarrow eX)}{\sigma(e^+e^- \rightarrow \mu^+\mu^-)}$  vs. the CM energy  $\sqrt{s}$  for all  $eX$  events with no detected photons [285]. The three fitted curves indicate the threshold behavior for different spins of  $\tau$ .

various values of spin  $J = 0, \frac{1}{2}, 1$ . It was inferred from Figure 5.17 and Eqs. (5.144)–(5.146) that

- i)  $\tau$  has a mass  $m_\tau = 1.784_{-0.0036}^{+0.0027}$  GeV.
- ii)  $\tau$  has spin  $\frac{1}{2}$ .
- iii)  $\Lambda > 50$  GeV implying that  $F(s) \approx 1.0014$ , that is,  $\tau$  is a point particle.

Therefore, it is concluded that the  $\tau$  particles called tauons are heavy leptons of spin  $\frac{1}{2}$ , like muons, and have their own  $\nu_\tau$  associated with them, since:

$$\tau^- \rightarrow e^- + \gamma \text{ or } \tau^- \rightarrow \mu^- + \gamma$$

decays have never been observed. The non-observation of these decays leads to a separate lepton number  $L_\tau$  for  $\tau$  and  $\nu_\tau$  leptons and their conservation law. It also establishes that there are three generations (flavors) of neutrinos, that is,  $\nu_e$ ,  $\nu_\mu$ , and  $\nu_\tau$ . The name ‘heavy lepton’ given to  $\tau$  leptons is a misnomer because the word ‘lepton’ is taken from Greek which describes something which is light.

### 5.8.2 Weak decays of $\tau$ leptons and $e - \mu - \tau$ - universality

The purely leptonic modes of  $\tau$  lepton are

$$\tau^- \rightarrow e^- + \bar{\nu}_e + \nu_\tau \quad (5.148)$$

$$\tau^- \rightarrow \mu^- + \bar{\nu}_\mu + \nu_\tau, \quad (5.149)$$

where  $\nu_\tau$  is the neutrino corresponding to  $\tau$ . These decays are like the muon-decays. In addition, the  $\tau$ , being a massive particle may also decay weakly into modes involving particles of higher masses like  $\pi, \rho$ , and  $K$ , through two particle and three particle decays like:

$$\tau^\mp \rightarrow \pi^\mp \nu_\tau (\bar{\nu}_\tau), \quad K^\mp \nu_\tau (\bar{\nu}_\tau), \quad \rho^\mp \nu_\tau (\bar{\nu}_\tau) \quad (5.150)$$

$$\tau^\mp \rightarrow \pi^\mp \pi^0 \nu_\tau (\bar{\nu}_\tau), \quad \pi^0 \rho^\mp \nu_\tau (\bar{\nu}_\tau), \quad \pi^\mp \nu_\tau (\bar{\nu}_\tau). \quad (5.151)$$

A list of dominant decay modes are given in Table 5.7. It may be noticed that the purely leptonic (hadronic) modes contribute about 35%(65%) of the total decay probability of the  $\tau$  lepton. If we assume that the  $\tau$  lepton behaves like a muon with the only difference being its mass, then the three-body decay can be calculated using the  $V - A$  theory. The energy spectrum of the emitted lepton in the limit  $m_l(l = e, \mu) \rightarrow 0$  and the decay rate  $\Gamma$  is then given by:

$$\frac{d\Gamma}{dE_e} = \frac{G_\mu^2 m_\tau^5}{192\pi^3} 2\epsilon^2 [3 - 2\epsilon] \left( \frac{1 - \hat{n} \cdot \hat{s}}{2} \right) d\epsilon, \quad (5.152)$$

**Table 5.7** Decay modes of tau lepton [117].

Mode	BR(%)
$e^- \bar{\nu}_e \nu_\tau$	$17.82 \pm 0.04$
$\mu^- \bar{\nu}_\mu \nu_\tau$	$17.39 \pm 0.04$
$\pi^- \nu_\tau$	$10.82 \pm 0.05$
$K^- \nu_\tau$	$(6.96 \pm 0.1) \times 10^{-3}$
$\rho^- \nu_\tau$	$(21.8 \pm 2.0)$
$\pi^- \rho^0 \nu_\tau$	$(5.4 \pm 1.7)$
$\pi^- \pi^0 \nu_\tau$	$25.49 \pm 0.09$
$e^- \bar{\nu}_e \nu_\tau \gamma$	$1.83 \pm 0.05$
$\pi^- 2\pi^0 \nu_\tau$	$9.26 \pm 0.1$
$K^- 2\pi^0 \nu_\tau$	$(6.5 \pm 2.2) \times 10^{-4}$
$\pi^- \pi^- \pi^+ \nu_\tau$	$9.31 \pm 0.05$
$\pi^- \pi^- \pi^+ \pi^0 \nu_\tau$	$4.62 \pm 0.05$

where  $\epsilon = \frac{2E_l}{m_\tau}$ ,  $E_l$  is the energy of the outgoing lepton and  $\hat{s}$  represents the spin of the outgoing lepton. Assuming the outgoing lepton to be left-handed, that is,  $\hat{n} \cdot \hat{s} = -1$ , we obtain:

$$\Gamma = \frac{G_\mu^2 m_\tau^5}{192\pi^3}. \quad (5.153)$$

This expression is obtained in the limit  $m_l = 0$ , where  $m_l$  represents the mass of the outgoing lepton ( $e^-$  or  $\mu^-$ ). Taking into account the lepton mass, the expression of the decay rate becomes

$$\Gamma = \frac{G_\mu^2 m_\tau^5}{192\pi^3} \left( 1 - 8\epsilon^2 - 24\epsilon^4 \ln(\epsilon) + 8\epsilon^6 - \epsilon^8 \right), \quad \text{where } \epsilon = \frac{m_l}{m_\tau}$$

The electron energy spectrum given in Eq. (5.152) is shown in Figure 5.18, where it is compared with the experimental results [133]. The agreement between the theory and the experiment is very good.

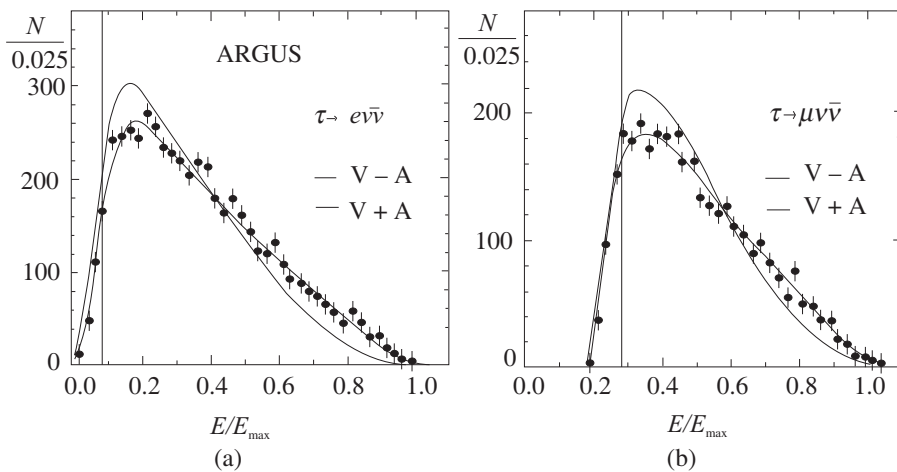


**Figure 5.18** Normalized (left) electron and (right) muon energy distributions for tau decays compared with V–A (solid line) and V+A (dashed line) spectra[286].

Using this result in  $V - A$  theory, we can also obtain:

$$\begin{aligned} \Gamma_{\tau^- \rightarrow e^- \nu_e \nu_\tau} &= \Gamma_{\mu^- \rightarrow e^- \bar{\nu}_e \nu_\mu} \left[ \frac{m_\tau^5}{m_\mu^5} \left( 1 - \frac{8m_e^2}{m_\tau^2} \right) \right] \\ \Gamma_{\tau^- \rightarrow \mu^- \nu_\mu \nu_\tau} &= \Gamma_{\mu^- \rightarrow e^- \bar{\nu}_e \nu_\mu} \left[ \frac{m_\tau^5}{m_\mu^5} \left( 1 - \frac{8m_\mu^2}{m_\tau^2} \right) \right] \\ \Rightarrow R = \frac{\Gamma_{\tau \rightarrow \mu}}{\Gamma_{\tau \rightarrow e}} &= \frac{\left( 1 - \frac{8m_\mu^2}{m_\tau^2} \right)}{\left( 1 - \frac{8m_e^2}{m_\tau^2} \right)}. \end{aligned} \quad (5.154)$$

Using the values of  $m_e$ ,  $m_\mu$ , and  $m_\tau$ , we obtain:

$$\begin{aligned}\Gamma_{\tau \rightarrow e} &= 0.620 \times 10^{12}/s \\ \Gamma_{\tau \rightarrow \mu} &= 0.603 \times 10^{12}/s \\ \text{and } R &= \frac{\Gamma_{\tau \rightarrow \mu}}{\Gamma_{\tau \rightarrow e}} = 0.972,\end{aligned}\tag{5.155}$$

which is in agreement with the experimental values of  $\frac{\Gamma_{\tau \rightarrow \mu}}{\Gamma_{\tau \rightarrow e}} = 0.9 \pm 0.1$ . Of course, the radiative corrections are different in all these cases as they are mass dependent and are large for  $\tau^\pm$  decays.

The Michel parameters  $\rho$ ,  $\eta$ ,  $\xi$ , and  $\delta$  determined experimentally from the analysis of the three particle weak decays of  $\tau$  leptons are shown in Table 5.8 along with theoretical predictions of  $V - A$  theory. The agreement between the theoretical and experimental values of the Michel parameters is very good. This shows that the weak interaction of  $\tau$  leptons have a  $V - A$  structure with the same coupling strength for the vector and axial vector currents as in the muon-decay which establishes the  $e - \mu - \tau$  universality of weak interactions.

**Table 5.8** Michel parameters of the  $\tau$  lepton [287].

Name	SM value	Experimental results [288]	Comments and Ref.
$\eta$	0	$0.013 \pm 0.020$	(ALEPH) [289]
$\rho$	3/4	$0.745 \pm 0.008$	(CLEO) [290]
$\xi\delta$	3/4	$0.746 \pm 0.021$	(CLEO) [290]
$\xi$	1	$1.007 \pm 0.040$	(CLEO) [290]
$\xi_h$	1	$0.995 \pm 0.007$	(CLEO) [290]